UNIVERSITA' DEGLI STUDI DI VERONA

DEPARTMENT OF
SURGERY, DENTISTRY, PAEDIATRICS AND GYNAECOLOGY

_____

DOCTORAL PROGRAM IN

Surgical and Cardiovascular Sciences – CV in Odontostomatologic Sciences

38° Cycle / year (3° year) _____

TITLE OF THE DOCTORAL THESIS

Digital Engineering and 3D Bioprinting for Bone Regeration: an Innovative Software for PEGDA Custom-Made Meshes

S.S.D. 26/D

Coordinator: Prof./ssa __Andrea Ruzzenente_____

Signature _____

Tutor: Prof./ssa _____Daniele De Santis___

Signature _____

Doctoral Student: Dott. Frensi Balliu

Signature _____

TABLE OF CONTENTS

PART III – DESIGN, DEVELOPMENT, AND EXPERIMENTAL VALIDATION OF PEGDA MEMBRANES

PART I – Introduction

"1.1 Guided Bone Regeneration (GBR) principles

Alveolar ridge atrophies represent one of the main challenges in implant rehabilitation, as they significantly compromise the structural, functional, and aesthetic outcomes of the treatment (Elgali I, 2017).
Alveolar bone loss may result from periodontal disease, trauma, tumors, or the prolonged absence of teeth.
In all these cases, it is essential to have an adequate bone volume at the time of implant placement to ensure predictable and long-lasting results.
Several surgical strategies have been proposed to compensate for bone deficiencies: onlay e inlay block grafting, maxillary sinus lift, ridge splitting, osteogenetic distraction and Guided Bone Regeneration (GBR).
In all of these cases, GBR was proven to be the most reliable technique in terms of stability of the regenerated bone volume, vertical incrementation, survival ratio and overall implant success (Elnayef B, 2017).
Guided Bone Regeneration is a surgical technique that employs barrier membranes for isolating soft tissues from the bone defect, allowing clot stabilization and creating a favorable environment for the migration and proliferation of che osteoprogenitor cells.
In oral surgery the membrane can be:

- **Resorbable**, such as those made of collagen or synthetic materials (polylactic-polyglycolic acid, polyethylene glycol-based polymers);
- **Non-resorbable**, such as expanded e-PTFE membranes or titanium meshes.

The aim of the membrane is to avoid the proliferation of non osteogenic tissue inside the defect, allowing so the colonization exclusively from bone cells.
The first clinical applications employed non resorbable membranes (e-PTFE), that needed a secondary surgical procedure for the removal of the membrane (Sasaki JI, 2021).

Subsequently, the development of collagen resorbable membranes consented to avoid this additional phase, simplifying the procedure (Ren Y, 2022).

Subsequently, the development of **resorbable collagen membranes** eliminated the need for a second surgical intervention, **thereby simplifying the overall procedure** (Elgali I, 2017).

The concept of **Guided Bone Regeneration (GBR)** emerged in the **1980s** as an evolution of the **Guided Tissue Regeneration (GTR)** approach used in periodontology. Dahlin C et al. were the first to demonstrate, in preclinical animal models, the potential for new bone formation in periodontal defects through the application of a **barrier membrane** (Dahlin C, 1988). Since then, the technique has been progressively refined and successfully extended to implant surgery, enabling **horizontal and vertical bone regeneration** in resorbed ridges. Today, GBR is widely acknowledged as a reliable and predictable procedure for the management of alveolar ridge atrophies. Implants placed in regenerated bone demonstrate survival rates comparable to those placed in native bone (Tay JRH, 2022)

Figure 1 - A) Shows the first generation of non-resorbable membrane comprising of a uniform e-PTFE stucture. (B) Shows a new dual configuration e-PTFE membrane with tailor-made surfaces facing the soft and hard tissues respectively. (Dahlin, 2017)

Over the following decades, advancements in **membrane design** and **grafting materials**, along with an enhanced understanding of the **biological mechanisms governing bone regeneration**, have significantly improved clinical outcomes. Nevertheless, **GBR remains a surgically demanding procedure** that requires meticulous attention to **membrane stability**, **flap management**, and the **prevention of postoperative complications**, particularly **early membrane exposure** (Tay JRH, 2022).

1.2 Biological Mechanism of GBR

Achieving predictable bone regeneration requires both advanced surgical proficiency and also a comprehensive understanding of the biological mechanisms underlying tissue healing.
According to the **P.A.S.S.** framework (Wang HL, 2006) ,four fundamental biological principles are essential for successful regenerative outcomes:

1. **Primary wound closure**, which preserves a stable environment for undisturbed healing;
2. **Angiogenesis**, ensuring an adequate blood supply and the recruitment of undifferentiated mesenchymal cells;
3. **Space maintenance or creation**, which provides sufficient room for new bone formation;
4. **Stability of the wound and graft**, promoting blood clot organization and consistent, complication-free healing.

The classical understanding of Guided Bone Regeneration (GBR) has been reshaped by recent advances in molecular biology have reshaped. The membrane is now recognized as a **bioactive component** that directly interacts with

surrounding tissues and cellular processes, originally it was conceived as a purely mechanical approach**:** a passive barrier preventing soft-tissue invasion into bone defects,

Modern research demonstrates that barrier membranes trigger specific biological responses depending on their surface properties such as topography, roughness, wettability, porosity, and chemical composition. These characteristics influence the adsorption of proteins, which in turn modulate the inflammatory and immune responses of host tissues (Hu WJ, 2001) (Tanaka S, 2007). Today we can analize the membrane not as an inert separator but we understand better its active regulatory role in wound healing and osteogenesis.

Studies have shown that both resorbable and non-resorbable membranes can stimulate molecular pathways associated with bone formation.

Increases in the expression of **Runx2/Cbfa1**, **osteocalcin** have been observed during the early healing stages beneath PTFE membranes. These findings suggest an upregulation of inflammatory mediators followed by a major expression of bone-forming genes as healing progresses (Tanaka S, 2007).

Similarly, collagen-based resorbable membranes have demonstrated the ability to upregulate genes such as **osteocalcin, cathepsin K, and RANKL**, indicating an active role in stimulating osteoblastic differentiation. Immunohistochemical and histologic analyses further confirm the presence of bone-specific proteins (**alkaline phosphatase, osteopontin, osteocalcin**) along the inner membrane surface, highlighting its bioactivity to promote bone neoformation (Al-Kattan R, 2017).

Although the benefits discussed above are noteworthy, one should also take into account the considerable heterogeneity of biological behavior of membranes remains heterogeneous differences in materials, fabrication techniques, and experimental models. Due to the complexity and the difficulty in comparing the available studies, further research **(**in vivo and clinical studies) is required to clarify these findings.

To assist in space maintenance during bone regeneration, **titanium meshes**—either customized or prefabricated—are often employed in combination with membranes.

Nonetheless, the stiffness supplied by the meshes often leads to its exposure and this can be detrimental for the regenerative outcome since it is associated with subsequent complications such as infection and significant graft resorption. Moreover, these titanium meshes alone without barrier membrane do not fulfil the principle of compartmentalization since there is no cell occlusion effect (Buser D, 2023).
Clinical data indicate that mesh exposure rates approach **20%**, exceeding those typically reported for vertical augmentation procedures using traditional GBR protocols (Urban IA, 2019).

1.3 Proprieties of membrane barriers

Etymologically, a membrane is defined as any thin pliable sheet of material, while a barrier is an object or layer that physically prevents something from moving from one place to another (Gabriel Mizraji, 2023). In the late 50s, the importance of space maintaining and barrier membranes was described for the treatment of spinal fusion (Hurley LA, 1959). Surgeons affirmed: "osteosynthesis in the spine was surely achieved if the paraspinal muscles were elevated from the decorticated laminae, creating a space in which bone-forming granulation tissue could grow."
Ideally, a new developed membrane should pass the cascades of evaluations from in vitro to clinical testing until being approved as medical devices according to current ISO standards and specifications.
Beyond its basic barrier function, an ideal membrane is required to exhibit several essential properties, including: biocompatibility, biological activity, porosity/occlusive properties, mechanical properties, exposure tolerance, and biodegradability (Mariano Sanz, 2019).

1. *Biocompatibility*: The biomaterial shall perform with an appropriate tissue response. Hence, the interaction between the material and the tissues

should not adversely affect the surrounding tissues, the intended healing result or the safety of the patient. (Williams, 2016).

2. *Biological activity*: Increasing evidence suggests that membranes contribute to bone regeneration not solely through their occlusive function, but also by actively stimulating biological processes within the underlying defect. This bioactivity may involve cellular recruitment, angiogenesis, new bone formation, and subsequent bone remodeling, ultimately resulting in defect fill with mature bone. Experimental data indicate that collagen membranes permit the inward migration of cells capable of expressing and releasing osteogenic and angiogenic mediators. However, it remains unclear whether membranes made of different materials exhibit comparable biological behaviors.
3. *Porosity/occlusive properties*: The optimal membrane porosity has not been defined yet. In the commercially available membranes for GBR there is a wide variability in the pore size and degree of permeability: micro-porosity (5–20 μm), may limit the passage of cells, but allows the passage of chemicals, biomolecules, viruses; moderate porosity (non-resorbable materials ≤100 μm) that also allows the passage of bacteria, cells and tissue integration/migration (tissue integration occurs ≥30–40 μm); macro-porosity (non-resorbable materials >100 μm) which allows unrestricted passage of chemicals, biomolecules, viruses, bacteria, cells and allows tissue integration and migration. During the process of membrane degradation within the tissue the pore size can increase, which may modify its bioactivity, passage of nutrient and cells and the ingrowth of nutrients and soft and hard tissue cells.
4. *Mechanical properties*: The ideal GBR membrane should be sufficiently rigid for an adequate space-making capacity and able to withstand the pressure of the overlying soft tissues during function in order to prevent its collapse. It should be combined with a bone replacement biomaterial/graft that serves as a scaffold, to attain the desire volume of regenerated bone. The membrane needs to be flexible and easy to handle and place correctly over the defect.

5. *Integration with the tissues*: The integration of the membrane with the adjacent connective tissues is essential for optimal primary wound closure and healing. In fact, lack of integration and membrane exposure is associated with inferior regenerative outcomes. The mobility of the membrane and absence of hydrophilicity will negatively affect connective tissue integration and bone formation. In case of non-resorbable membranes, the degree of tissue integration should be coupled with an easy and atraumatic removal.
6. *Exposure tolerance*: complication that occurs when the protective barrier becomes visible through the overlying soft tissue, which can happen with both resorbable and non-resorbable membranes. This exposure can significantly reduce the amount of bone regenerated, often due to bacterial colonization that leads to an inflammatory response, compromising the graft's success. Management varies based on factors like the timing of exposure, size, and condition of the underlying tissue, and may involve conservative measures or surgical intervention.
7. *Biodegradability*: The longer the membrane maintains its function the greater the maturity of the bone is. The ideal membrane bio-absorption time has not yet been established. The inflammatory response elicited by the degradation of the membrane should not adversely affect the regenerative outcome.
8. Antibacterial proprieties: Traditionally, commercial chemical drugs such as metronidazole, amoxicillin, and ammonium chloride have been loaded into dental membranes for sterilization (Inoue BS, 2020) (He M, 2020). These drugs inhibit bacterial deoxyribonucleic acid (DNA) synthesis and metabolism. Despite their prominent antibacterial properties, these drugs have gradually been replaced due to side effects, such as the development of bacterial strain resistance. Recently, researchers have incorporated metals such as copper (Cu), Ag, and Zn ions into membranes to enhance antimicrobial properties (Shan Y, 2024) (Nasajpour A, 2018). These metals can eliminate bacteria by producing reactive oxygen species (ROS), such as singlet oxygen ($^1O_2$), superoxide ($O_2^{\cdot -}$), hydrogen peroxide (H_2O_2),

and hydroxyl radicals (·OH) (Qi K, 2017). Drug resistance can be avoided using these metals and their compund.

1.4 Surgical Techniques for Alveolar Bone Regeneration

The reconstruction of alveolar bone in the implant site represents a key step in oral implantology.

Numerous clinical techniques have been developed for the restoration of alveolar bone defects, including Guided Bone Regeneration (GBR), onlay grafts, bone expansion methods, split-crest procedures, and distraction osteogenesis (Table 1).

Thanks to its operational simplicity, osteogenic stability, and multidirectional bone formation capacity, *Guided Bone Regeneration (GBR)* has become one of the most widely used techniques for the repair of alveolar bone defects.

Thanks to its operational simplicity, osteogenic stability, and multidirectional bone formation capacity, *Guided Bone Regeneration (GBR)* has become one of the most widely used techniques for the repair of alveolar bone defects.

The procedure typically involves flap elevation, precise defect debridement, placement of a particulate bone graft, and coverage with a membrane that prevents soft tissue invasion while maintaining the regenerative space. The membrane is then stabilized to ensure immobility, followed by tension-free primary wound closure to allow undisturbed healing. This approach facilitates osteogenic cell migration and controlled bone regeneration within the protected area (Rispoli, 2015).

Surgical Techniques

Expansive Techniques	Split Crest Summers Osteotomes Edentulous Ridge Expansion
Additive Techniques	Onlay Grafts Inlay Grafts Revascularized Grafts
Displacement Techniques	Sinus Lift NAI Repositioning Le Fort I OSBAM (Gotte Method)
Tissue Engineering Techniques	Bone Distraction GBR Cell Cultures
Combined Techniques	Le Fort I with Inlay Grafts NAI Repositioning with Onlay Grafts

Table 1 Pre-prosthetic surgical techniques for bone augmentation

1.5 CBR®: Evolution of GBR Concept

Three-dimensional (3D) technology has enabled the development of **Customized Bone Regeneration (CBR)**, a new approach in guided bone regenerative surgery (GBR). This personalized technique is tailored to the patient's specific clinical needs and anatomical characteristics, based on individualized digital design criteria.

The fabrication of **Yxoss CBR® membranes** (Geistlich Biomaterials), following the evaluation of DICOM data obtained from CBCT scans, involves CAD/CAM design and 3D printing, allowing for the regeneration of extensive alveolar ridge defects—whether vertical, horizontal, or combined—while significantly reducing surgical time.

Thanks to their precise adaptation to the defect morphology, these patient-specific titanium meshes can be positioned without intraoperative manual shaping, effectively eliminating sharp edges and irregular contours that might generate shear forces and mucosal irritation. This precision reduces the risk of wound dehiscence, mesh exposure, and failure of the regenerative procedure.

In the augmentation of bone defects, the final bone structure is an important success factor in order to achieve the highest esthetic standards. Positional stability and shape are of the highest priority for the selected bone augmentation material.

The individually shaped Yxoss CBR® titanium scaffold enable a stability and accuracy of fit of the previously planned augmentation volume that was unknown in augmentation procedures before.

"Part of this section has been adapted from the author's previously published thesis on customized bone regeneration using Yxoss CBR® titanium meshes (University of Verona, 2021). The content has been revised and expanded for the purposes of this doctoral dissertation."

1.5.1 Previous Research Experience: Customized Titanium Mesh System (Yxoss CBR®)

Customized titanium meshes (Yxoss CBR® – Geistlich Biomaterials) are non-resorbable, patient-specific membranes designed to regenerate complex alveolar bone defects.
They are fabricated by combining CBCT data with 3D printing technology, allowing precise adaptation to the individual anatomy of each patient.

Figure 2 Yxoss CBR - Geistlich Biomaterials

The manufacturing process is divided into the following stages:

1. Selective laser sintering (SLS)
2. Surface treatment (sandblasting)
3. Sonic cleaning treatment (ultrasonic bath) and sterilization in autoclave

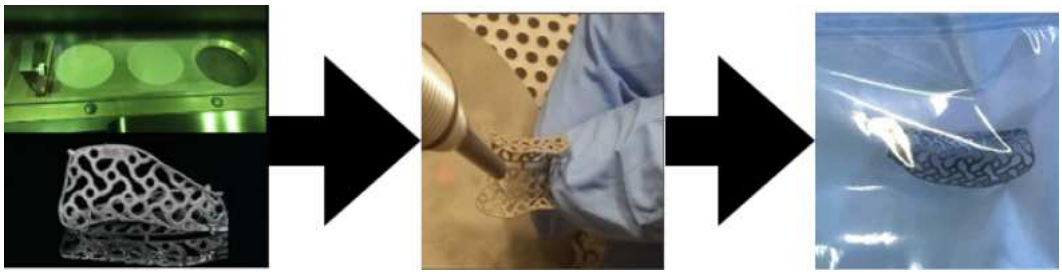

Figure 3 - Manufacturing process of Yxoss CBR® meshes

Yxoss CBR® is used for the reconstruction of alveolar bone defects prior to implant placement, for the modeling of the alveolar ridge, and for supporting the

regenerated bone volume in cases of bone defect regeneration, which may include:

- extraction sites,
- horizontal and/or vertical augmentation of the alveolar ridge,
- reconstruction of maxillofacial bone defects.

We have different morphologies of titanium meshes, designed according to specific clinical indications to enable the surgical rehabilitation of complex bone defects. In particular, the following product line is currently available on the market:

Figure 4 Yxoss CBR® Configurations

The *Yxoss CBR® Classic* configuration is designed with an open structure. The wide lattice geometry consent periosteal vascularization and nutrient diffusion, enabling faster bone maturation and enhanced defect mineralization.
The *Yxoss CBR® Protect* is designed with a Dual-structure. The open architecture of the upper region allows periosteal blood supply. The denser microstructure of the apical region reduces tissue infiltration.
The *Yxoss CBR® Fully Protect* is designed with a homogeneous fine microstructure across the entire surface preventing excessive tissue adhesion.

Prevents soft and hard tissue penetration, providing simplified and predictable membrane removal.

"Adapted from Geistlich Biomaterials, Yxoss CBR® product information (accessed 2025)."

1.5.2 Advantages

The rigidity of *Yxoss CBR*® titanium meshes provides excellent stabilization of both the bone graft and the blood clot, maintaining the necessary space for regeneration and ensuring volumetric stability in three dimensions.
Yxoss CBR® therefore enables predictable volumetric bone augmentation and supports the regeneration of complex bone defects. *Yxoss CBR*® membranes offer predictable and reproducible clinical outcomes thanks to their precise adaptation to the patient's bone anatomy and their high level of tissue compatibility.
They allow a perfect fit to both the bone defect and the residual alveolar ridge, defining the contours of the area to be regenerated and serving as a precise reference for subsequent implant placement.
Customized membranes significantly reduce surgical time, as they are self-retentive and require minimal intraoperative manipulation.
Fixation is simple and quick, while removal is facilitated by the Easy Removal Design, which includes pre-defined cutting points specifically engineered to allow the easy detachment of the mesh at the end of the healing phase.

Figure 5 Easy Removal Design: pre-defined cutting points

The clinical efficacy of Yxoss CBR® membranes was confirmed by a study conducted on 17 patients and 21 treated sites (Sagheb, 2017).
The study reported an average vertical bone gain of 6.5 mm and a horizontal gain of 5.5 mm, with an implant survival rate of 100% after a follow-up period of approximately 12 months.

1.5.3 Surgical Procedure for Customized Bone Regeneration (CBR®)

INCISION

The initial incision must be designed according to the extension and the location of the region to be augmented, respecting the following anatomical structures: maxillary sinus, nerves, vessels and ligaments. A flap with a wide base ensures adeguate blood supply. It is important to consider the also the periodontal conditions of adjacent teeth and their prosthetic support.
The healing process is influenced positively by the realization of a Full-Thickness Flap, avoiding tissue compression during the mobilization of the flap and a marginal incision, especially in aesthetic area.
When the mesh is inserted, the periosteum and the flap must not be damaged or perforated, and the mobilization of the flap must be clean and undermining.
The incision is generally performed to allow for a tension-free closure of the flap after mesh placement, taking into account the increased volume expected in situ.

The flap design can be performed according to two main approaches:

1) Crestal Incision Technique
2) “Poncho” Incision Techinque

CRESTAL INCISION TECHNIQUE

A crestal incision of mucosa and periosteum is performed, extending over 3-4 teeth distally (if possible). The flap design is full thickness and there are not releasing incisions (De Santis, 2021).

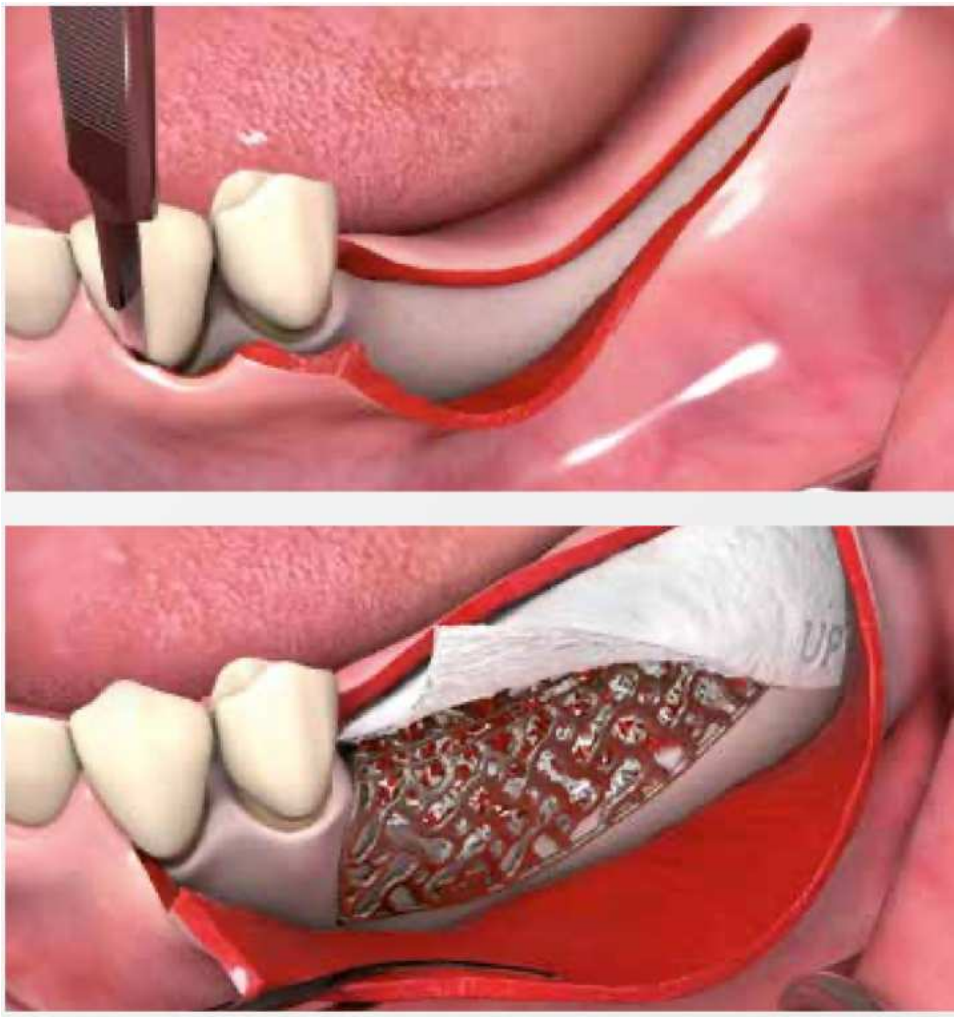

Figure 6 Crestal Incision Technique

When the mesh is positioned and the augmentation is performed according to the GBR principles, the flap can be mobilized with a the flap can be further mobilized through a deep periosteal-releasing incision in the vestibular area to ensure a tension-free closure.

PONCHO TECHNIQUE

A vestibular incision of the mucosa, muscle and periosteum is performed, then the flap is prepared and mobilizated. No releasing incisions are made and the flap design is full-thickness (De Santis, 2021).

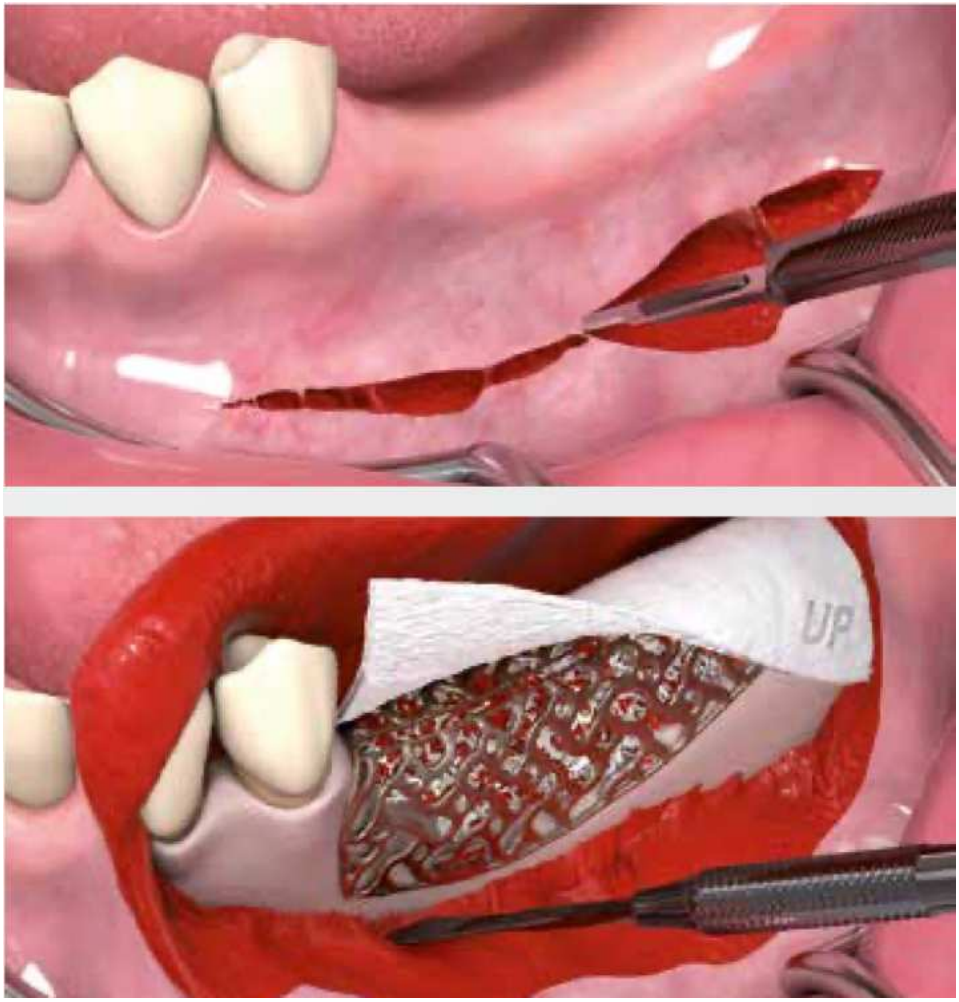

Figure 7 Poncho Incision

Poncho technique is preferred in extended vertical defects. After the incision a muco-periostal flap is performed, scar tissue is removed and the defect is exposed.

SURGICAL SEQUENCE

The surgical sequence can be divided into three main phases:
preparation of the defect, bone grafting procedure for augmentation, and subsequent closure of the surgical site.
In the anterior region, a marginal incision is performed without releasing incisions, while in non-esthetic areas a “poncho” incision is preferred.
The following steps include the preparation of a mucoperiosteal flap, debridement of the fibrotic tissue, and exposure of the defect. The underlying bone at the implant site is smoothened.
In one-stage procedures, implants are placed simultaneously, with or without the use of a surgical guide. Primary stability of the implants must be ensured, paying particular attention to the correct position of the implant shoulder in relation to the cemento-enamel junction of the adjacent teeth.
Passive and tension-free adaptation must be achieved during the trial fitting of the customized Yxoss CBR® mesh, maintaining biological distances (1.5 mm from adjacent teeth or neural structures)
After harvesting intraoral autogenous bone, the graft material is prepared in particulate form. The titanium mesh is then filled with a 50:50 mixture of homologous and heterologous bone and adapted to the atrophic site.
This combination allows the osteogenic and osteoinductive properties of autogenous bone to be integrated with the scaffold function of the xenograft.
The fixation and stabilization of grid is achieved by osteosynthesis screws inserted into the residual bone through the mesh perforations, following the principles of mechanical stability and minimal stress. A resorbable membrane is positioned over the mesh to prevent soft-tissue ingrowth and to support soft-tissue regeneration.

The connective tissue should be tightly sutured using a tension-free suture over the titanium mesh. The wound must be closed by primary intention to minimize the risk of inflammatory reactions in the surgical area.

RE-OPENING AND REMOVAL OF THE YXOSS CBR® MESH

After suture removal and throughout the entire healing phase, the condition of the soft tissues should be regularly monitored clinically to check for any dehiscence or inflammatory signs. After an appropriate healing period (approximately one year), the Yxoss CBR® mesh can be removed.
For mesh removal, the same initial incision (poncho technique) is recommended. After raising the mucoperiosteal flap, an increase in well-vascularized tissue volume and possible osteoblastic proliferation through the mesh can be observed. After unscrewing the fixation screws, the mesh can be carefully removed.
Yxoss CBR® features predefined fracture points to allow an easy removal of the titanium grid. The mesh can be mobilized using lateral extrusion movements without compromising the regenerated volume.
The surgical wound can be closed tension-free with interrupted sutures or combined with mucosal grafts to increase the amount of keratinized gingiva. Suture removal is performed after one week.

PROSTHETIC TREATMENT

Maintaining proper hygiene of provisional restorations is essential. Pressure on the regenerated tissues must be avoided to prevent adverse effects on the obtained bone regeneration. Otherwise, the definitive restoration should be postponed in cases of poor patient compliance.
The final prosthesis is fabricated according to conventional prosthetic protocols.

1.5.4 Clinical Case Series

The surgical procedures were performed at the Department of Maxillofacial Surgery and Dentistry, G.B. Rossi University Hospital, Verona.
The study included 16 patients (14 treated and 2 scheduled for treatment), with a total of 17 customized titanium meshes designed and **15 of them already surgically placed**. Among these, **14 meshes were evaluated radiographically** with both pre- and post-operative CBCT analysis.
A total of **21 implants** were placed in **10 patients** who had completed the regenerative phase. Specifically, **11 implants were placed in the maxilla** (5 in the pre-maxilla and 6 in the posterior sectors), and **10 implants in the mandible**, all located in posterior regions. The distribution revealed a predominance of posterior sites, consistent with the higher prevalence of complex resorptive defects in these regions. This anatomical distribution reflects the indication of customized titanium meshes in posterior alveolar ridge augmentation, where vertical and combined bone deficiencies are more frequent and challenging to treat.
A poncho flap incision was designed in all the 15 performed surgery in order to avoid titanium mesh exposure or deiescence.
A total of **17 alveolar defects** were regenerated.
In all cases, a 50:50 mixture of autologous and heterologous bone was used as grafting material.
All surgical procedures were performed under local or regional anesthesia.

"The following page shows the clinical and surgical experience gained through the use of customized titanium meshes (Yxoss CBR®). The observation of the clinical case series has played a fundamental role in shaping the current research direction.
Deeper understanding of the biological behavior of bone regeneration in relation to customized titanium barriers, including their handling, fixation stability, and soft-tissue response has been achieved from this experience.
Far from representing a stand-alone study, this part of the study represents the foundation and natural continuation of our research pathway on guided bone regeneration."

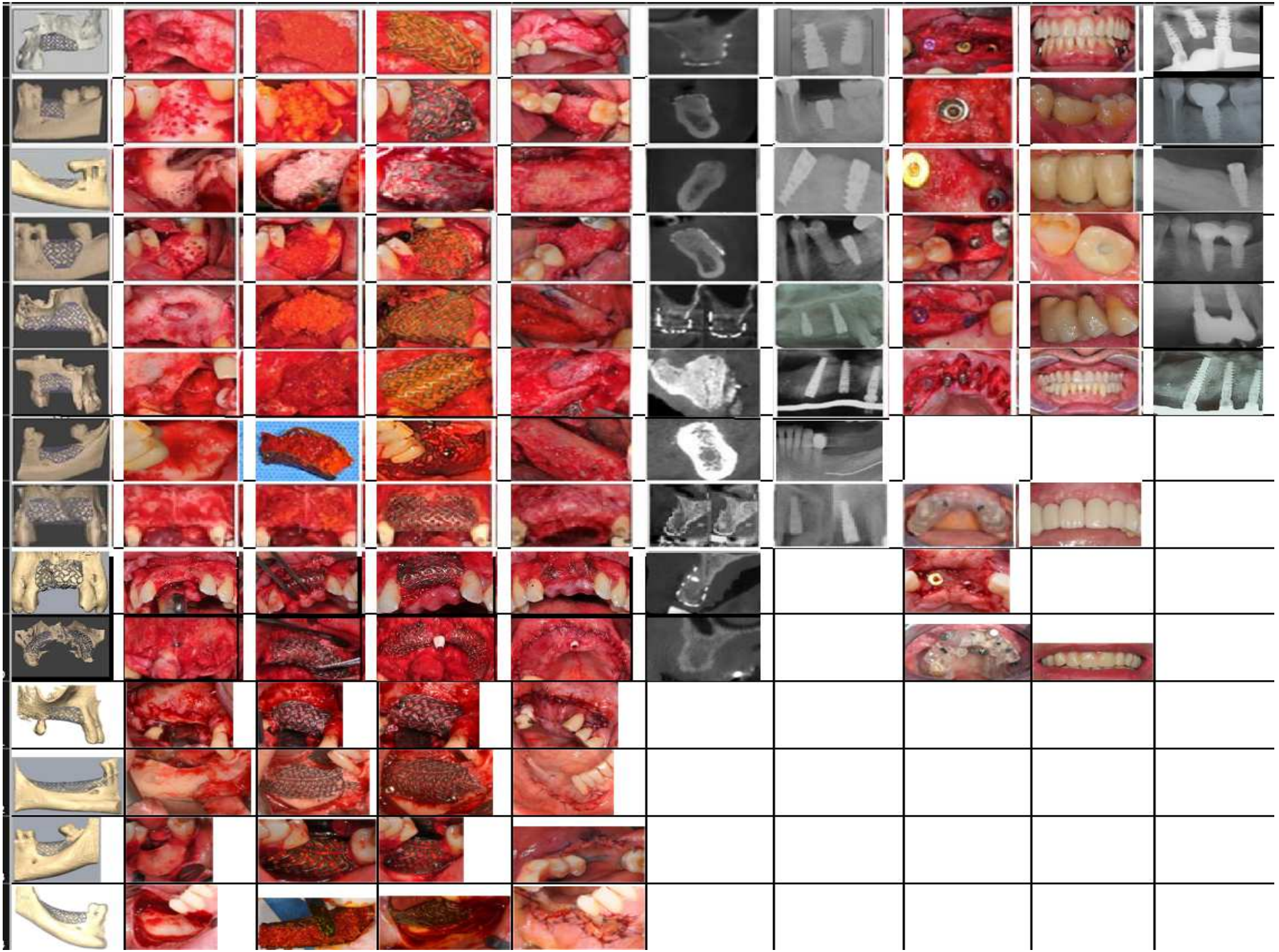

Table 2 Summary table of patients treated with Yxoss CBR®

RESULTS

The post-operative was uneventful in the majority of the cases, with an average mean healing period of 8-9 months. This period consented in most patients the simultaneous implant placement with the removal of the customized titanium mesh, according to the Customized Bone Regeneration (CBR) protocols.
Partial mesh and localized exposure of the mesh was observed in two cases (12.5%), non surgical treatment was performed by means of Chlorhexidine (0,2%) medication and strict clinical follow-up.
None of the exposures resulted in graft loss or compromised regenerative process.
Pre- and postoperative radiographic measurements (CBCT) showed a significant increase in bone volume, both horizontally and vertically.
In the 14 cases analyzed with complete measurements, the following results were obtained:

- Mean horizontal gain: 3.1 ± 1.13 mm
- Mean vertical gain: 4.7 ± 1.94 mm

The data are consistent with the reference literature which reports mean horizontal and vertical increases of 4.33 ± 0.57 mm and 4.83 ± 0.89 mm, respectively, in similar cases treated with Yxoss CBR® meshes (De Santis D, 2021).
The comparability of the results confirms the effectiveness and predictability of three-dimensional regeneration using customized meshes, with stable and uniform integration of the newly formed bone tissue.
Overall, 21 implants were placed in the regenerated sites.
At the clinical and radiographic follow-up evaluation, 20 implants were found to be fully osseointegrated and functional, with a survival rate of 95.24%.
The implants showed good maintenance of marginal bone levels and no signs of peri-implantitis or dehiscence. Only one implant showed marginal crestal resorption, which was not clinically significant.
Soft tissue management was a key factor in treatment success. In all cases, closure was achieved by primary intention, using single interrupted sutures and deep mattress stitches, avoiding tension on the flap.
The planned flap design, combined with the choice of incision technique, allowed for predictable and stable coverage of the titanium meshes.

The overall exposure rate observed was 15.38%, lower than the average values reported in the literature.

As described by Sagheb et al. (2017), crestal incisions present an exposure risk of up to 45.5%, while the "modified poncho" technique reduces this risk to around 20%.

In the present study, thanks to the prevalent use of the "poncho" technique, the exposure rate was further reduced (15.38%), confirming the greater reliability of this surgical approach in CBR.

From a clinical standpoint, no serious infections or dehiscences occurred.

The formation of a vascularized fibrous tissue over the mesh was observed in several cases: this tissue, with a granular appearance and similar to the periosteum, played a protective role for the graft, preventing bacterial contamination and excessive resorption.

This phenomenon known as “pseudo-periosteum” was observed by Von Arx (1998, 1999) who hypothesized a biological origin associated with the maturation processes of the regenerated tissue (Malchiodi L, 1998).

The pseudo-periosteum was considered the connective tissue between the regenerated bone and barrier device. The pseudo-periosteum was clinically assessed and divided into three types (Cucchi A, 2019) to facilitate classification using the Murphy system, which evaluates utility, adequacy, disjointedness, and simplicity (Pini-Prato 2011):

- Type 1: no pseudo- periosteum or a layer of soft tissue thinner than 1 mm;
- Type 2: a regular soft tissue layer between 1 and 2 mm;
- Type 3: an irregular layer of soft tissue and/or a layer thicker than 2 mm.

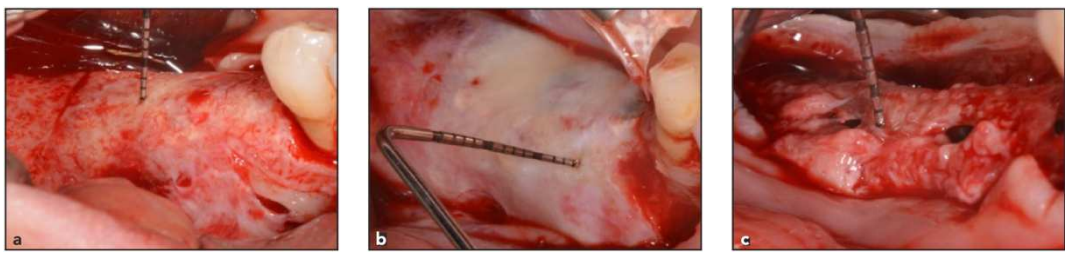

Figure 8 ***Classification of pseudo-periosteum:*** **(a)** ***Type 1 with tissue < 1 mm;*** **(b)** ***Type 2 with regular tissue between 1 and 2 mm; and*** **(c)** ***Type 3 with irregular tissue > 2 mm. (Cucchi A, 2019)***

Postoperative CBCT analysis confirmed the volumetric and morphological stability of the newly formed tissue, with regular and continuous bone profiles.
No mesh collapse or loss of regenerated volume was observed.
The bone density observed in the treated areas was homogeneous and compatible with the surrounding bone, confirming the quality of the regeneration achieved.
The results obtained (Table 2) demonstrate that customized bone regeneration using the Yxoss CBR® titanium mesh represents a predictable, stable, and safe technique for correcting complex three-dimensional bone defects.
Excellent soft tissue control, combined with the precision of digital design, allows for reproducible results over time.
Furthermore, the data confirm that this method is not an isolated experiment, but fits coherently into the broader research path on guided bone regeneration and the evolution of titanium membranes, which continues to be the subject of clinical and experimental investigation.

Patient No.	Sex	Age	Site	Initial Width	Initial Height	Final Width	Final Height	Horizontal Gain	Vertical Gain	Number of Implants	Implant Survival	Exposure
1	F	43	22-23-24	2,8	2,2	6,1	9,9	3,3	7,7	3	Si	No
2	F	51	36	4,2	6,2	8,9	11,1	4,7	4,9	1	Si	No
3	F	62	13-11-23-24	3,8	9,1	7,1	11,2	3,3	2,1	2	Si	No
4	F	51	36	3,1	8,2	7,3	11,6	4,2	3,4	1	Si	No
5	F	48	11-12-13-14	4,9	5	10,7	11,9	5,8	6,9	3	Si	No
6	M	49	14-15-16	3,2	4,1	6,4	9,5	3,2	5,4	2	Si	No
7	F	49	36	8,1	6,3	9,7	10,2	1,6	3,9	/	/	No
8	M	55	46	6,2	6,9	8,3	8,2	2,1	1,3	2	1	No
9	M	58	12-13-14-15	4,2	3,2	5,6	9,3	1,4	6,1	2	Si	Si
10	M	58	22-23-24-25	4,2	3,2	5,6	9,3	1,4	6,1	3	Si	No
11	F	38	11-12.	3	2,8	6,5	9,1	3,5	6,3	2	Si	Si
12	M	59	14-15-16	3,4	4,3	6,8	9,7	3,4	5,4	/	/	/
13	M	64	44-45-46-47	5,8	5,9	8,1	8,4	2,3	2,5	/	/	/
14	F	48	36-37	4,6	6,1	8,3	9,5	3,7	3,4	/	/	/
15	F	60	45-46-47-48	6,5	4,7	/	/	/	/	/	/	/
16	F	60	34-35-36-37-3	6,1	5,6	/	/	/	/	/	/	/
17	F	44	22-23	2,7	2,1	/	/	/	/	/	/	/
				sum	sum	sum	sum	Mean Horizontal Gain	Mean Vertical Gain	Total	Survival %	Exposure %
				61,5	73,5	105,4	138,9	3,1	4,7	21	95,24%	15,38%

Table 3 Summary of cumulative and mean values for horizontal and vertical bone gain, implant survival, and exposure rates

DISCUSSION

The clinical outcomes obtained in the present study are consistent with the main findings reported in the current literature on guided bone regeneration using customized titanium meshes. Although the mean horizontal (3.1 ± 1.13 mm) and vertical (4.7 ± 1.94 mm) gains were slightly lower than those reported (De Santis et al. 2021), (Corinaldesi G, 2017), (Chiapasco M, 2021), the results remain within the expected range of predictability for complex three-dimensional bone defects. These variations can be attributed to the heterogeneity in defect morphology, anatomical location, and the differences in mesh design or fixation protocol among studies (Table 4.).

The use of a mixed graft material in a 1:1 ratio of autologous to heterologous bone appeared to provide a favorable balance between regenerative potential and volumetric stability. This approach aligns with the findings of (Troeltzsch M, 2016), who demonstrated improved bone density and space maintenance when autologous bone was combined with xenogenic material. The heterologous component, with its slower resorption rate, appears to counterbalance the rapid remodeling of autogenous bone, supporting long-term stability of the regenerated volume.

Vertical augmentation proved to be more demanding and sensitive to flap management and mechanical stability. However, the presence of a rigid, digitally designed mesh structure likely contributed to the maintenance of the desired volume and to the prevention of collapse under soft tissue pressure. This finding is in agreement with the data of (Sagheb et al. 2017), (Ciocca L, 2019), confirming that 3D-printed meshes enhance structural reliability compared to manually adapted titanium barriers.

The exposure rate observed in this study (15.38%) was lower than the average reported in conventional GBR procedures, supporting the protective role of digital customization and the “poncho” flap design in reducing dehiscence and infection risk. Moreover, the occurrence of a vascularized connective tissue layer, referred to as pseudo-periosteum, further supports the biological integration of the graft. As previously described by Von Arx (1998, 1999) and later classified by (Cucchi A S. M., 2019), this tissue likely acts as a functional interface between the

regenerated bone and the soft tissue, promoting long-term stability and resistance to exposure.

Overall, the present findings confirm that digitally customized titanium meshes, when combined with careful flap management and a balanced graft composition, represent a predictable and clinically safe protocol for the reconstruction of complex alveolar defects. The consistency of these results with previous clinical studies strengthens the evidence supporting the ongoing evolution of the CBR approach within the broader framework of titanium-based guided bone regeneration.

STUDY	*HORIZONTAL GAIN (mm)*	*VERTICAL GAIN (mm)*	*MEAN HORIZONTAL GAIN (mm)*	*MEAN VERTICAL GAIN (mm)*
Corinaldesi et al. 2007	5,4	4,2	4,33	4,83
Pieri et al. 2008	3,71	4,16		
Proussaefs & Lozada 2006	3,75	2,56		
K. Sagheb 2017	5,5	6,5	1,63	2,81
Ciocca 2018	3,41	4,57		
Miyamoto 2012	3,7	5,4		
Raisa-Dal Polo 2014	4,36	4,91	0,57	0,89
Chiapasco 2021	4,78	6,35		

Table 4 Mean bone gain reported in the literature for GBR procedures using titanium meshes

MANAGEMENT OF EXPOSURES

The exposures observed were classified based on the timing of onset:

1. Immediate exposure (within 1 week): Mesh removal is recommended to prevent contamination, with minimal loss of bone gain and the possibility of implant placement (Rasia-dal Polo M, 2014).
2. Early exposure (2–3 weeks): Preservation of the membrane is recommended, as the regenerative process has already begun (Miyamoto I, 2012).
3. Late exposure (>3 weeks): Mesh preservation is recommended, as bone integration is already at an advanced stage (Sagheb 2017), (Belleggia F, 2023).

In both exposure cases observed in the study, conservative management was chosen, which allowed for complete healing of the soft tissue and volumetric stability of the regenerated tissue.

It was found (Kaya, 2025) that dehiscence in augmentations using customized titanium meshes is primarily associated with smoking status and defect location in the maxilla. Early detection and prompt management of dehiscence are essential to optimize clinical outcomes. No significant correlation was found between gingival phenotype and the occurrence of dehiscence ($p = 0.495$). However, the slightly higher dehiscence rate observed in patients with a thin phenotype may be attributed to reduced stability and a higher risk of tearing during the titanium mesh placement and wound closure (Hartmann A, 2020). The literature also suggests that a thin phenotype type is significantly more challenging to handle intraoperatively compared to a thick one. Larger procedures involving significant alveolar defects may pose a higher risk for dehiscence due to prior manipulation and subsequent weakening or scarring of the soft tissue (Hartmann A H. H., 2019).

1.5.5 Limitations

Customized Titanium Meshes require a second-stage surgery**.** They are non-resorbable, after 12 months of bone healing they must be surgically removed. The increases the patient's discomfort.

Customized titanium meshes have lower risk conventional meshes due to smoother, pre-formed edges.

Exposure of the mesh through the gum tissue is a significant risk. Exposure can lead to infection and potential graft failure. The success of CBR relies on careful soft tissue management to ensure a tension-free, complete primary closure over the mesh. Inadeguate soft tissue coverage can lead to exposure.

When the mesh is removed, a layer of connective tissue (pseudo-periosteum) may be found on the regenerated bone surface, which indicates some level of soft tissue infiltration. Soft tissue ingrowth can lead to minor bone augmentation ratio (Xie Y, 2020).

Digital workflow (CBCT, CAD/CAM design, 3D printing), can lead to higher cost of the surgical procedure for the patient. 3D planning and manufacturing process accuracy is very important for the success of the customized mesh (Cirrincione, Guarnieri, & Morelli, 2025).

Errors in the virtual design or an imprecise fit could compromise the regeneration outcome. The learning curve is very important for the clinician to interpret the 3D planning data for optimal mesh design.

The increased rigidity, which could potentially cause mechanical stress on the overlying soft tissue flap if not managed correctly (M.C. Mateo-Sidrón Antón, 2025).

1.5.6 Conclusion of the Clinical Case Series and Introduction to the Experimental Phase

Within the limitations of the present study, the findings indicate that the use of individualized bone regeneration (CBR) with 3D customized titanium meshes fabricated through CAD/CAM technology represents a safe and predictable approach for the reconstruction of complex bone defects.
This technique offers a reliable alternative in cases where conventional regenerative methods may not provide adequate support or stability.
The design of the flap and the achievement of a tension-free primary closure remain the most delicate steps of this digitally guided procedure. Proper soft-tissue management is essential to prevent wound dehiscence and ensure optimal integration of the graft.
Partial exposure of the titanium mesh does not necessarily compromise the regenerative process. Most authors agree that the incidence of exposure is significantly lower when the "poncho" flap design is used instead of a crestal incision. The "poncho" approach can therefore be considered a protective factor for the grafted area, helping to maintain tissue integrity and favor bone healing.
Furthermore, the adoption of a fully digital workflow—especially the preoperative planning phase—appears to enhance the clinical reliability of the procedure. Careful virtual design and surgical precision contribute to minimizing intraoperative risks, improving the predictability of outcomes, and supporting a more standardized and reproducible approach to customized bone regeneration (CBR).
The intrinsic limitations identified such as the need for a second-stage removal surgery, potential mesh exposure, and the absence of resorption capacity reveals the necessity of developing next-generation regenerative materials that combine mechanical stability, biocompatibility, and controlled resorption.
This clinical experience represents not only the scientific validation of the Customized Bone Regeneration (CBR) concept but also the conceptual foundation for the next phase of this research."

“This prior work forms the scientific starting point and motivation for developing novel, resorbable and printable membrane systems that preserve the precision of titanium meshes while overcoming their biological and clinical limitations.”

The first part of this study builds upon the author’s previous dissertation, authored by Dr. Frensi Balliu: “Rigenerazione ossea guidata con una nuova griglia in titanio customizzata”; and has been updated with long-term follow-up data collected over several years.

The subsequent section of this dissertation is dedicated to the experimental and technological phase of research in development and characterization of PEGDA based 3D-printed membranes

PART II - SCIENTIFIC CONTEXT AND LITERATURE FRAMEWORK

2.1 Bone Tissue Engineering Approaches

Tissue engineering was defined by Langer and Vacanti in 1993 (Langer R, 1993), as a new approach which "applies the principles of biology and engineering to the development of functional substitutes for damaged tissue". In contrast to the traditional biomaterials approach at that time, this nascent field integrated knowledge across a diverse set of disciplines with the goal of inducing regeneration of damaged tissues rather than performing replacement with inert parts. It is a science based on fundamental principles that involve the identification of appropriate cells with the ability to differentiate into specialized regenerative cells, certain signaling molecules required to induce cells to regenerate a tissue or organ, and a conductive scaffold with vascular networks to provide nutrition for tissue growth. In the last few years, medicine has begun to explore the possible applications of stem cells and tissue engineering toward the repair and regeneration of body structures (Farah Shaikh, 2023).
Accordingly, tissue engineering triad combines three key elements:

- Stem cells
- Scaffold or supporting matrix
- Signaling molecules.

2.1.1 Stem Cells

Tissue regeneration requires specialized cells capable of synthesizing the extracellular matrix specific to each tissue. In this sense, stem cells have been extensively used in regenerative medicine (Moro JD, 2018).
They can be isolated from various sources, such as fetuses, embryos, or adult tissues, and their differentiation capability depends on the cell source.
Based on their characteristics (Rodríguez-Lozano FJ, 2012), stem cells can be classified into:

- Totipotent: these are embryonic cells and extra-embryonic cells, which can be differentiated into all cell types.
- Pluripotent: cells that can give rise to all the cell types that make up the body; except extra embryonic tissues such as placenta. For example, embryonic stem cells and induced pluripotent stem cells.
- Multipotent: these cells can develop into more than one cell type, which can give rise to tissues belonging to only one embryonic germ layer (ectoderm or mesoderm or endoderm), for example, cord blood stem cells and adult stem cells
- Clonogenicity: a stem cell is clonogenic as it can proliferate to form colony of cells.

Depending on the developmental stages of the tissues from which the stem cells are isolated, stem cells are broadly divided into embryonic stem cells and adult stem cells.

2.1.2 Scaffolds

The scaffold is a three-dimensional structure that serves as a template or framework for cell attachment, growth, and regeneration of new tissue. The purpose of a scaffold in tissue engineering is to provide a temporary framework for cells to attach and grow, and to mimic the natural extracellular matrix (ECM) that surrounds cells in the body.

Scaffolds can be fabricated using a variety of techniques, such as electrospinning, 3D printing, lyophilizing, phase separating, foaming, rapid prototyping, and microfabrication, and can be tailored to match the specific mechanical, chemical, and biological properties of the target tissue (Farah Shaikh, 2023).

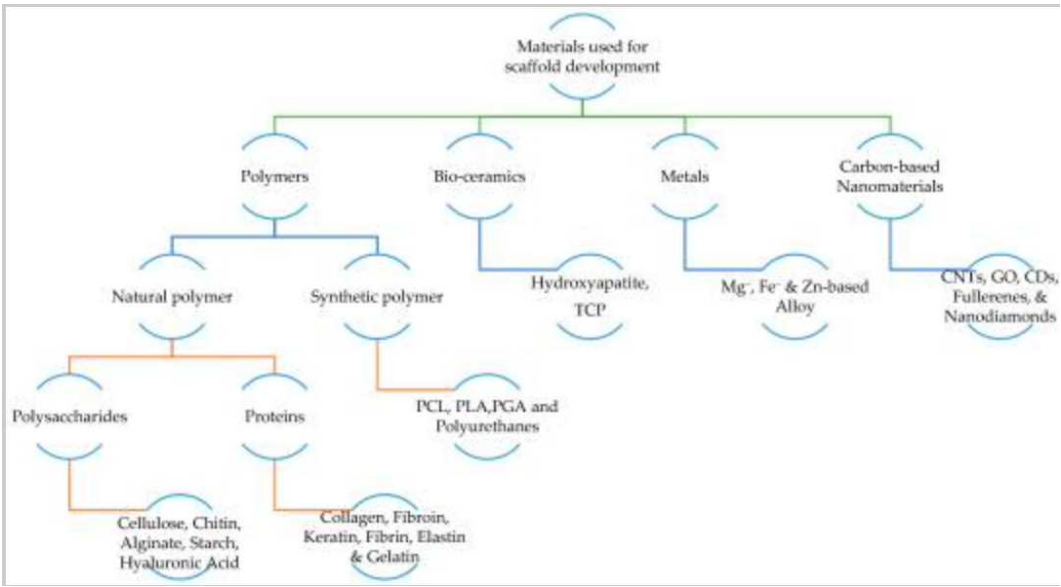

Figure 9 Scaffold Materials (Krishani M, 2023)

Biopolymers are also known as natural polymers. Natural polymers are materials that can be obtained from natural sources. They can be categorized into protein-based biomaterials (naturally occurring polymers in the human body such as collagen, fibrin, and elastin) and polysaccharides-based biomaterials (such as silk, chitosan, alginate, and gelatin). They exhibit similar characteristics to soft tissues, showing bioactivity, excellent cell adhesion and growth, and fulfilling biodegradability and biocompatibility. Moreover, they are also known for their wide availability, ecological safety, and modifiability to suit different applications. However, natural sources indicate the requirement of a purification step to avoid foreign immunological responses after implantation (Krishani M, 2023).

The commonly used chemical compounds to fabricate synthetic scaffolds include poly(a-hydroxyester) s, polyanhydrides, and polyorthoesters. Among these polymers, poly(a-hydroxy- ester)s such as polylactide (PLA), polyglycolide (PGA), and its copolymers are extensively used. These polymers are biocompatible, biodegradable, bioresorbable, and can be easily processed to form various 3-D structural Poly Lactic-co-Glycolic acid (PLGA) copolymers with controlled degradation matrices (Gunatillake PA, 2003).

Ceramic materials obtained from natural products, termed bio-ceramics, have been widely used in dental and bone tissue engineering. Bio-ceramics are organic, non-metallic solids with good compatibility, bio-inertness, bioactivity, osteoconductivity, and mechanical strength (Perić Kačarević Ž., 2019). Human bone and teeth are composed of an inorganic compound known as hydroxyapatite, which constitutes calcium, phosphate, and OH radicals with high tensile strength and quickly adheres to host tissues. Many studies revealed that HAp is non-toxic and lacks inflammatory and pyrogenetic response (Sabir A., 2021).

Biodegradable metals are metals having controlled corrosion properties. They can be grouped into pure biodegradable metals (Mg^{-}- and Fe^{-}-based), biodegradable alloys, and biodegradable metal matrix composites (Sultana N., 2015). Biodegradable metals overcome problems such as innate immune rejection and have good load-bearing capacity during bone healing. However, biodegradable metals such as Mg and their alloys have a high corrosion rate.

Researchers have integrated nanotechnology with tissue engineering to design carbon-based nanomaterial scaffolds with improved functional and structural characteristics. Various carbon nanomaterials—including carbon nanotubes (CNTs), graphene oxide (GO), carbon dots (CDs), fullerenes, and nanodiamonds—have been explored as scaffold components in tissue engineering applications. These materials exhibit several advantageous properties, such as high biocompatibility, mechanical robustness, minimal cytotoxicity, and the ability to promote cellular communication and nutrient transport, making them highly suitable for scaffold fabrication and regenerative purposes (Ku S.H., 2013).

2.1.3 Signaling Molecules:

Growth factors refers to soluble, secreted signaling polypeptides or proteins, which can be synthesized by a wide variety of cells and play an important role in the regulation of cell proliferation, migration, differentiation, and ECM synthesis (Tessmar, 2007). Growth factors usually exhibit short-range diffusion through the ECM and act locally.

Bone morphogenetic proteins (BMPs), vascular endothelial growth factor (VEGF), and platelet-rich plasma (PRP), induce stem cell differentiation and promote angiogenesis (blood vessel formation), which is crucial for bone regeneration.

Endocrine secretion molecules (e.g. hormones) are a class of signaling molecules, produced by glands in multicellular organisms, transported by the circulatory system, and then targeting distant organs to regulate physiology such as tissue growth, function, and development (Potts, 311–325). o reach their potential in promoting tissue regeneration, these molecules need to be delivered at specific time points and follow a certain release pattern (Chertok, 2013). For example, parathyroid hormone (PTH) is a hormone that is crucial to regulating bone remodeling, where bone tissue is alternately resorbed and rebuilt over time (Qin, 2004).

Nucleic acids alter cellular function and modulate the tissue regeneration process at the genetic level. DNAs and mRNAs encoding for growth and differential factors can enable protein expression for an extended period of time (Franceschi, 1093–1103). For example, genes encoding for BMPs, FGF-2, insulin-like growth factors (IGFs), TGF-β, platelet-derived growth factor (PDGF), and VEGFhave been shown to induce bone regeneration (Dang, 2018).

2.1.4 Bone Tissue Engineering Application

Bone tissue engineering (BTE) has become an integral component of various oral and maxillofacial surgical procedures.
In ridge preservation and augmentation, grafting materials are applied following tooth extraction to preserve alveolar bone dimensions, ensuring adequate height and width for subsequent implant placement.
Maxillary sinus floor augmentation, commonly known as a sinus lift, is performed to restore bone volume in the posterior maxilla when vertical bone height is insufficient due to resorption or close proximity to the maxillary sinus.
For reconstruction of extensive defects, BTE plays a critical role in restoring bone continuity in cases resulting from trauma, tumor resection, or congenital deformities such as cleft palate.
Finally, in periodontal regeneration, BTE approaches are employed to restore bone and periodontal support structures compromised by advanced periodontal disease.

2.1.5 Novel Applications of Bone Tissue Engineering

In the field of Tissue Engineering and Regenerative Medicine, a promising effective technology for generating bio-artificial tissue and organ-like structures through an automatic layerwase deposition is an additive manufacturing commonly referred to as 3D Bioprinting (Mojdeh Mirshafiei, 2024). Through 3D bioprinting, biomaterials, bioactive molecules, and cells are located layer-by-layer with accurate spatial control (Q. Zhang, 2022). Thereby, patient-specific constructs or implants with hierarchical organization and high resolution can be easily fabricated using medical images or computer design to replicate the intricate geometry and irregular shapes of native tissue (G. Größbacher, 2023). To achieve a successful 3D bio-printed tissue, factors that affect the functionality and integrity of resulting bio-printed constructions, i.e. design, technology, and material selection, should be considered.

Injectable Biomaterials such as Hydrogels and calcium phosphate cements can be injected and harden in place. They allow for less invasive procedures and better adaptation to irregular shapes. Hydrogels are highly hydrated three dimensional (3D) polymeric networks that are stabilized by crosslinks of various natures (N. Annabi, 2014). The hydrated volume of hydrogels can easily enable the encapsulation of water-soluble drugs, especially macromolecular proteinaceous drugs, without adversely compromising the therapeutic efficacy of the drugs (T.R. Hoare, 2008).

Bone cements are injectable and self-setting materials that are widely used in hard-tissue repair, such as in orthopedics, orthodontics, and plastic surgery. This category of injectable biomaterials usually undergoes a transition from the fluid or viscous state that can be readily injected through needles or a cannula to the solidified state that possesses a fixed geometry with increased mechanical strength and stability. Currently, acrylic cements, such as polymethyl methacrylate (PMMA), have become clinically standard augmentation materials for hard tissues and are injected into patients in millions of procedures conducted worldwide every year (Huan Zhou, 2019).
Secretome-based therapies have emerged as a promising alternative to cell-based therapies. The ability to be manufactured, stored, and used as off-the-shelf ready-to-go products while maintaining the therapeutic benefits of stem cells but with fewer safety concerns have situated the secretome at the forefront of next-generation tissue and organ-regenerative engineering applications (Daneshmandi L, 2020). The secretome is defined as the repertoire of molecules and biological factors that are secreted from cells into the extracellular space. These secretory factors play important roles in many biological functions, including homeostasis, development, signaling, immunomodulation, inflammation, angiogenesis, apoptosis, proteolysis, adhesion, and extracellular matrix (ECM) organization (Konala, 2016). The secretome comprises various serum proteins, growth factors, angiogenic factors, hormones, cytokines, ECM proteins and proteases, and even in low abundance, lipid mediators, and genetic material. It is broadly categorized into soluble factors (growth factors, cytokines, chemokines,

and enzymes) and extracellular vesicles that transport lipids, proteins, and RNA and DNA subtypes. The composition of the secretome is dynamic, depending on the cell type and microenvironmental stimuli. However, generally, the stem cell secretome is known to have therapeutic benefits for tissue repair including proangiogenic, antiapoptotic, antifibrotic, anti-inflammatory, and immunomodulatory effects (Haque, 2018).

Smart-Biomaterials have received increasing attention from researchers in recent years. Rapid progress in the manufacture of smart stimuli-responsive biomaterials has occurred in the past 5 years, from applying external stimulation to enhance bone regeneration and therapeutic effects for smartly responses to variations in the internal microenvironment to rational synergistic therapy combining multiple strategies to improve therapeutic efficacy (Wei, 2022). There are recognized four levels of smartness: inert, active, responsive, and autonomous. According to the clinical features smart biomaterials can respond to internal material properties (e.g., topography, mechanical properties, surface charge, and scaffold chemistry) or to external stimuli (e.g., piezoelectricity, magnetism, pH, and enzymes).

2.2 Conventional Membranes

Membranes are fundamental in guided bone regeneration (GBR), specially due to their capacity to separate the bone defect from the surrounding connective and epithelial tissues. The underlying principle is based on selective cell repopulation allowing osteogenic cells to occupy the defect while preventing the faster migration of fibroblasts and epithelial cells.

In regenerative surgery membranes are categorized into non-resorbable and resorbable membranes.

Non-resorbable membranes provide excellent mechanical stability and space maintenance but have the major disadvantage of requiring a second-stage surgery for removal. Moreover, their exposure rates and susceptibility to bacterial contamination are relatively high, often compromising regenerative outcomes.

Resorbable membranes were developed to overcome these drawbacks, eliminating the need for a second surgery. They exhibit good biocompatibility, promote soft tissue integration, and gradually degrade through enzymatic processes. However, they lack sufficient rigidity to maintain large defect spaces and may collapse under soft tissue pressure (Dahlin, 2017).

2.2.1 Non-Resorbable Membranes

Non- Resorbable Membranes
e-PTFE (Goretex®)
d-PTFE (Cytoplast®)
Titanium-Reinfored e-PTFE (De Ore®)
Non-Customized Tianium Meshes
Customized Titanium Meshes

Table 5 Non-Resorbable Membranes

e-PTFE

The first synthetic polymer used in GBR procedures was expanded polytetrafluoroethylene (**e-PTFE**). This material, developed in 1969, became the standard for bone regeneration procedures during the early 1990s (Dahlin, 1990). The e-PTFE membranes are sintered with pore diameters ranging from 5 to 20 μm within the material structure. The most widely used commercial type of e-PTFE is the Gore-Tex® membrane.

e-PTFE resists enzymatic degradation by host tissues and does not elicit immunological reactions (Elgali, 2017).

Its chemical stability ensures the membrane's integrity and its barrier function, preventing soft tissue invasion into the grafted site.

However, membrane exposure in the oral cavity can lead to bacterial colonization and infection, potentially compromising both bone regeneration and implant osseointegration.

d-PTFE

Dense PTFE membranes (d-PTFE), due to their high density, provide enhanced bacterial resistance but are more prone to exposure because soft tissue cells cannot adhere or integrate effectively with their surface.

In two separate studies (Hoffmann O, 2008), (Barboza EP, 2010) including a total of 696 extraction sites, no cases of infection were reported when using high-density PTFE membranes (Cytoplast™ PTFE) following an open-healing technique.

Thanks to their Regentex™ TXT-200 microtextured surface, d-PTFE membranes exhibit a porosity that increases the effective surface area by 2.5 times, promoting cellular adhesion and reducing exposure risk while maintaining the principle of bacterial and soft tissue exclusion.

This enhanced surface area contributes to greater soft tissue stability and integration, which may further reduce the risk of membrane exposure.

According to Lee (Lee, 2010), there is no statistically significant difference in regenerated bone volume between e-PTFE and d-PTFE membranes. Similarly, no

significant differences were observed in marginal bone resorption after functional loading between the two types of PTFE membranes.

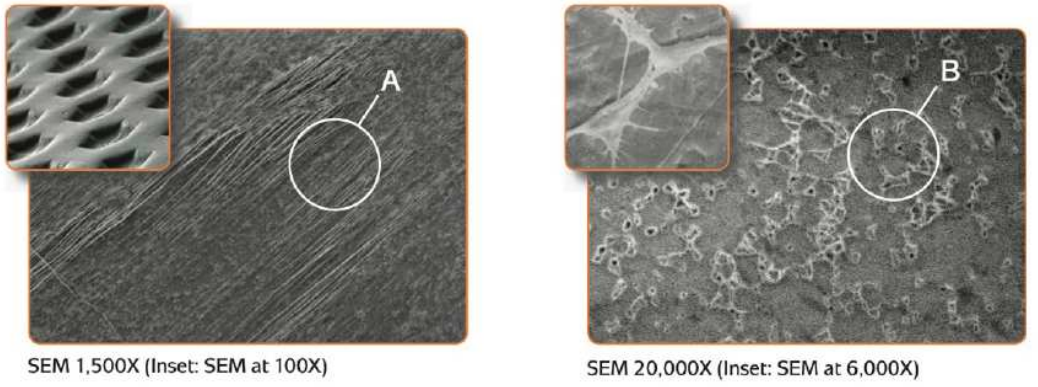

Figure 10 Ultrastructural detail of Cytoplast Membrane (SEM image - Biohorizons)

Titanium-reinforced e-PTFE

Figure 11 - e-PTFE Membrane (De- Ore Biomaterials)

Titanium-reinforced e-PTFE membranes are considered the **gold standard** for vertical bone regeneration procedures (Cucchi A G. P., 2014).
They combine the barrier function of e-PTFE with the mechanical support of a titanium framework, allowing space maintenance and preventing graft compression during healing.
The e-PTFE membranes show circular macropores that promote direct contact between the graft and the periosteum, facilitating cellular infiltration and vascularization.
Given that the rationale behind GBR membranes is space maintenance, titanium reinforcement allows the membrane to withstand soft tissue pressure while promoting bone maturation and corticalization over a healing period of approximately nine months.
Owing to its flexibility, the titanium-reinforced e-PTFE membrane achieves optimal adaptation to surrounding tissues.
In a clinical study by (Canullo L, 2008) involving ten cases with a follow-up of 24 to 54 months, an average vertical bone gain of 5.3 mm was reported using titanium-reinforced e-PTFE meshes combined with bovine bone grafts.
These findings further confirm the predictability and long-term success of this material in GBR techniques aimed at vertical ridge augmentation.

Non-customized titanium meshes

Figure 12 Non-Customized Titanium Mesh (Bionnovation Biomedical)

Non-customized titanium meshes provide excellent separation and protection of the underlying regenerated bone due to their rigidity.
They are easily shaped and adapted to the defect morphology and maintain their form over time once molded.
However, this modeling phase is typically performed intraoperatively, after graft placement, which extends surgical time and increases both patient discomfort and the risk of morbidity.
Alternatively, titanium meshes can be pre-shaped on stereolithographic models derived from the patient's maxillary anatomy prior to surgery, significantly reducing operative time and simplifying the clinical procedure (Di Stefano DA, 2019).

Customized Titanium Meshes

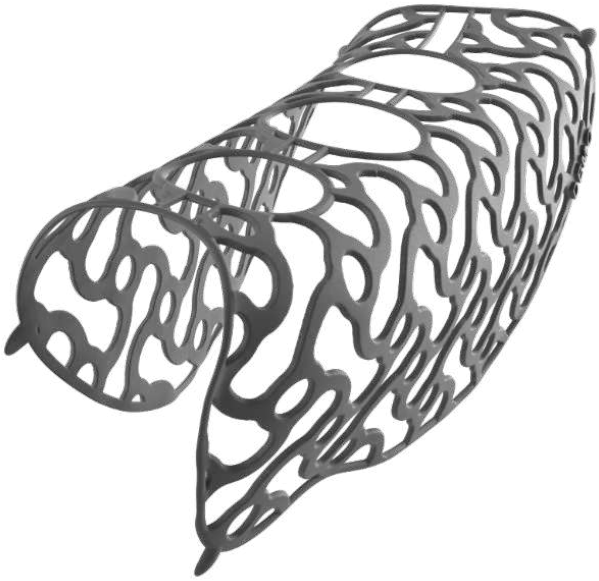

Figure 13 Yxoss - CBR (Geistlich Biomaterials)

Customized titanium membranes represent the most recent evolution in guided bone regeneration (GBR) technology.
Through digital planning (CAD) and computer-aided manufacturing (CAM),

these membranes are designed directly on the patient's three-dimensional bone defect obtained from CBCT or intraoral scans, ensuring a perfect anatomical adaptation and optimal space maintenance.

Unlike manually shaped meshes, customized membranes significantly reduce intraoperative time, improve precision and fit, and minimize the risk of soft tissue irritation caused by sharp edges or improper adaptation.

Clinically, these systems have shown predictable outcomes in both horizontal and vertical bone augmentations, with high stability of the regenerated tissue and a reduced incidence of postoperative complications.

However, despite their excellent mechanical performance, customized titanium membranes remain non-resorbable, requiring a second surgical procedure for removal, which can increase patient morbidity and overall treatment time.

SLM printing technique works with a laser source that melts the titanium powder alloy following the CAD project (N. Otawa, 2015), (D. Zhao, 2022) and one of the most important aspects related to the obtained product is the post-production process, which may alter or anyway modify the final roughness of the device surface, with important clinical and biological implications (N. Angelis, 2021), (N. Angelis, 2022).

Another important aspect is the thickness; infact traditional meshes are produced with an average thickness of 0,3mm, while customized devices are thicker (from 0,5mm to 0,8mm according to the manufacturer). As discussed above, the layer of soft tissues used for the surgical closure is extremely thin and represented only by the epithelial part, thus an unexpected trauma or simply a sudden movement of the lip or the chin may generate tension on the flap, which can easily relapse (N. Angelis, 2023).

2.2.2 Resorbable Membranes

Resorbable Membranes	
Natural	*Synthetic*
Xenogenic Collagen Type I or III	Polyurethane
	Polyglactin 910
	Polylactic acid
	Polyglycolic acid
	Polyorthoester
	Polyethylene glycol
	Different combinations of polylactic acid and polyglycolic acid

Table 6 Resorbable Membranes

Resorbable membranes are dived in Natural and Synthetic membranes:
Natural membranes include xenogenic type I or type III collagen membranes, which find wide application in guided bone regeneration (GBR) and guided tissue regeneration (GTR) procedures. These membranes are mainly derived from pericardium, dermis, or tendons and are of bovine or porcine origin (Lee J. S., 2020). Generally, they are produced through the isolation of the collagen fraction, purification, and precipitation by modifying ionic strength, pH value, or by increasing temperature, followed by an evaporation step in air. Finally, the purified collagen is lyophilized and sterilized. The degradation of collagen occurs enzymatically through specific proteases known as collagenases.
In GBR procedures, it has been demonstrated that covering the augmentation area with a collagen membrane (Geistlich Bio-Gide®) further reduces bone tissue resorption .

Polyurethane membranes are synthetic membranes containing organic polymers with multiple urethane groups (-NH-CO-O-). Polyurethanes are degraded

enzymatically and oxidatively (Matinlinna, 2014). They tend to expand after placement; moreover, inflammation and tissue recession phenomena are more pronounced than in poly-lactic membranes.

Polyglactin 910 fibers, a copolymer of glycolide and L-lactide (polyglycolide/polylactide, 9:1), form a tightly woven mesh used to produce Vicryl Periodontal Mesh®. The membrane begins resorption two weeks after placement, losing its structural integrity, and completely resorbs after approximately four or more weeks (Vert, 1992). Although animal studies indicate a lack of tissue integration and the formation of recessions, clinical evaluations suggest comparable efficacy to other membranes used in GTR procedures.

Polyglycolic acid (PLG) degrades rapidly (about two months), while polylactic acid (PLA), being more hydrophobic, persists longer (up to twelve months). When combined as copolymers, the time and degree of resorption depend on their ratio. The PLA/PLG copolymer is available in powder, gel, and sponge forms; the granules and powder of polylactic and polyglycolic acids are more osteoconductive than the gel version. The latter is currently used in combination with other heterologous materials due to its aggregating action, which makes it easier to handle (Robert, 1993).

Polyorthoester membranes, such as polydioxanone (PDO), are composed of a colorless, crystalline, resorbable polymer consisting of multiple ether–ester repeating units. They have shown promising results in tissue engineering due to their biocompatibility, low inflammatory response, and long resorption time (Saska, 2021).
PDO membranes undergo slow hydrolytic degradation, leading to the excretion of their metabolites via renal pathways, digestion, or exhalation as carbon dioxide.

Polyethylene glycol (PEG) is a biocompatible, cell-occlusive polymer widely used in GBR and GTR procedures. PEG hydrogel has demonstrated high biocompatibility and excellent tissue integration in rats, where degradation was

found to depend on PEG composition. Recently, PEG membranes have been shown to exhibit significant potential for bone augmentation procedures in large alveolar defects and for maintaining the crestal profile (Wang, 2016).

2.3 Additive manufacturing technologies

Additive manufacturing has revolutionized manufacturing across a spectrum of industries by enabling the production of complex geometries with unparalleled customization and reduced waste. Beginning as a rapid prototyping tool, additive manufacturing has matured into a comprehensive manufacturing solution, embracing a wide range of materials, such as polymers, metals, ceramics, and composites. T he process involves adding material layer by layer to create objects from 3D model data, contrary to traditional subtractive manufacturing methods. The overall pipeline of AM encompasses several critical steps, each contributing to the final product's accuracy, quality, and functionality. Each step in the AM pipeline is vital for ensuring that the final product meets the desired specifications and quality standards. Advances in software, materials, and printing technologies continue to expand the possibilities of what can be achieved with 3D printing, making it an increasingly integral part of modern manufacturing processes. (Zhou, et al., 2024).

Description	*Additive Manufacturing*	*Traditional manufactoring*
Prototype production	Does not need any special tooling in making parts	Need special tools to make parts
Waste prevention	Incredibly resource-efficient	Consumes a lot of resources
Large-scale production	Produces parts at speed	Less efficient and reliable
Presence of specific materials	Ability to make objects out of metallic polymers	No ability to make objects out of external materials
The scale of produced Parts	Restricts to a total area of the printing bed	Manufactures certain larger parts
Customization	Incredible use of small one-off production runs	Need for several tooling
Cost	Cost keep falling	Not easy to get started
Waste end energy	Saves on material wast and energy	No ability to add a material unit part
Inventory	Does not need much hands-on inventory	Need for a lot of hands-on inventory
Legacy Parts	Easy to recreate and optimize parts	Inability to recreate or to optimize legacy parts.

Table 7 Key difference between AM and traditional manufacturing (Saquib Rouf, 2022)

The first step of the typical process for three-dimensional (3D) printing of biomedical products is creating 3D models which is provided by obtaining the images from conventional computer-aided design (CAD) modelling of a patient through medical data capture methods such as magnetic resonance imaging (MRI), and computed tomography (CT). The second step is converting the data obtained from the patient into a 3D virtual model using CAD software. Then, the model is exported as a digital file, usually in the stereolithography (STL) file format. The STL file data is then sliced to create a series of two-dimensional (2D) layers, where each layer represents a cross-section of the 3D virtual model. Using the resulting 2D sliced data, the AM machine repositions materials, biomolecules, and even living cells layer-by-layer with extreme precision to produce 3D objects. These objects may require post-processing to remove support materials or improve structural properties in some cases. The development of biocompatible and printable materials makes AM technologies increasingly useful in different clinical applications (Celik HK, 2022).

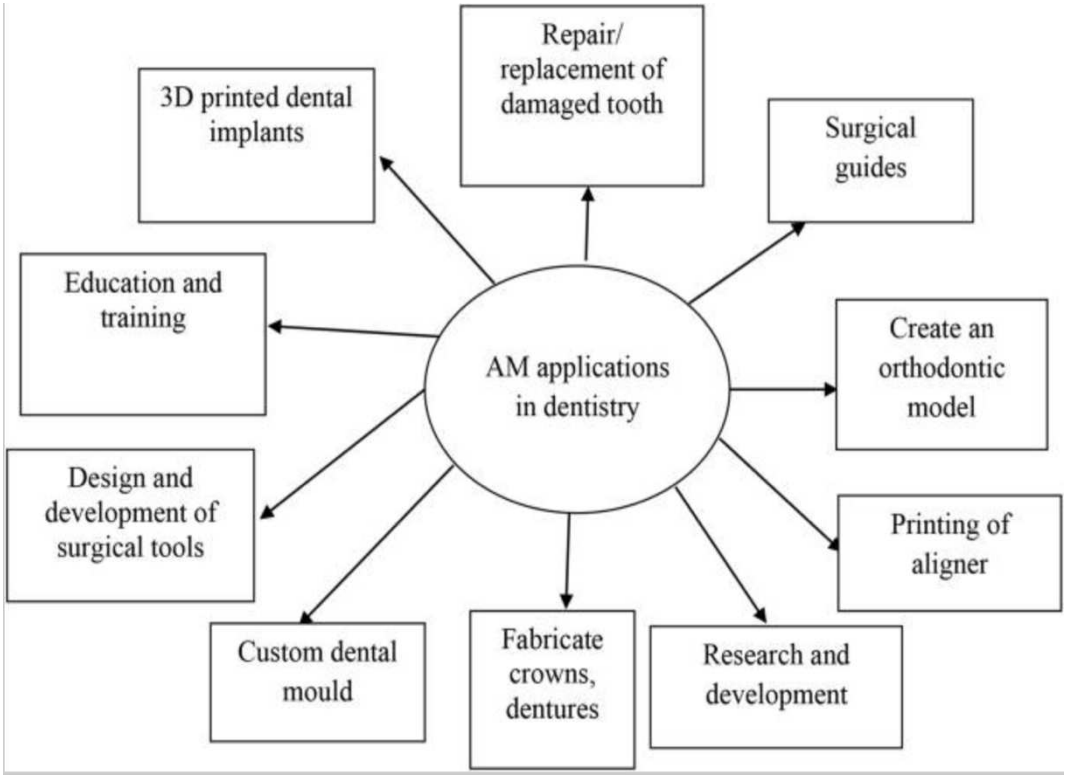

Figure 14 AM Applications in Dentistry (Javaid M, 2019)

Additive manufacturing technologies (AM) techniques such as fused deposition. Modelin (FDM), stereolithography (SLA), digital light processing (DLP), and bioprinting enable the fabrication of three-dimensional structures through a layer-by layer deposition process. The material extrusion family process, fused deposition modeling (FDM), is the most common type of printing used in medical or dental equipment; however, its printing resolution is inferior to that of SLA (Huang Y., 2017). FDM can handle a variety of materials, such as foundry wax, polyamide (commonly known as nylon), acrylonitrile butadiene styrene plastic, polylactic acid (PLA) plastic, low melting point metals, and ceramics (Lin et al., 2019). In FDM, the thermoplastic material is heated, melted, and extruded uniformly from a nozzle to generate filaments. Simultaneously, the nozzle moves along a specific path, operated by an NC system according to the continuous thin layer data planned by the slicing software, for filling. After cooling, the filamentous material is bonded layer by layer to form a thin cross-section, and finally the layers are superimposed to form a three-dimensional entity (Torabi K., 2015).

In SLA and DLP a liquid resin is selectively cured through polymerization mechanism (using a laser or projected light).

SLA is a well-known 3D printing technology that has been used for almost 30 and is primarily applied to print surgical guides, dental model replicas, custom trays, and provisional restorations. SLA uses a high-intensity ultraviolet light source, which applies the wavelength and heat of light to polymerize and selectively solidify liquid resin for lamination. In this process, to better integrate new layers with previous layers, the polymerization reaction of each layer is usually not fully completed under the direct light source, but further light processing is rather performed after the printing is completed. Finally, the support structures added automatically by the printer require manual removal (Huang S, 2023). A major area of DLP printer application is the digital manufacture of dental models (Park J. M., 2020). Differences between DLP and SLA include the type of light source and the way the light source is controlled to selectively illuminate and cure the resin. In SLA, the light source is a laser, while DLP uses a projector, similar to a movie projection device, that illuminates the entire shape of

the printed object at the surface of the liquid (Son K., 2021). DLP is advantageous for rapid printing of larger parts with fewer details, while SLA is superior for printing accurate parts with intricate details (Huang G., 2022) DLP offers printing efficiency by polymerizing an entire layer simultaneously. Bioprinting employs bio-inks composed of living cells and biomaterials to generate tissue-like constructs, with applications in regenerative medicine and tissue engineering. Bioprinting is an emerging technology with various applications in making functional tissue constructs to replace injured or diseased tissues. During the bioprinting process, a solution of a biomaterial or a mixture of several biomaterials in the hydrogel form, usually encapsulating the desired cell types, termed the bioink, is used for creating tissue constructs. This bioink can be cross-linked or stabilized during or immediately after bioprinting to generate the final shape, structure, and architecture of the designed construct. Bioinks may be made from natural or synthetic biomaterials alone, or a combination of the two as hybrid materials. In certain cases, cell aggregates without any additional biomaterials can also be adopted for use as a bioink for bioprinting processes. An ideal bioink should possess proper mechanical, rheological, and biological properties of the target tissues, which are essential to ensure correct functionality of the bioprinted tissues and organs (Gungor-Ozkerim PS, 2018).

AM Technologies	Process	Material	Applications
FDM (Fused Deposition Modeling)	A thermoplastic filament is heated and extruded through a nozzle, layer by layer, to build the object	Typically uses filaments of various polymers like ABS, PLA, or PETG.	Prototyping, creating tools, and functional parts, often favored for its lower cost.
SLA (Stereolithography)	A UV laser selectively traces and cures a layer of liquid photopolymer resin in a vat	A UV laser selectively traces and cures a layer of liquid photopolymer resin in a vat.	Prototyping with high detail and smooth surfaces, and producing parts requiring high accuracy.
DLP (Digital Light Processing)	Similar to SLA, but uses a digital projector to cure an entire layer of resin at once, resulting in faster print times.	Photopolymer resins	Rapid prototyping, high-resolution parts, and applications requiring both speed and detail.
BIO-PRINTING	Uses 3D printing techniques to build structures with bioinks, which are materials containing living cells.	Bioinks often consist of natural hydrogels and living cells.	Creating tissue models, scaffolds for tissue regeneration, and ultimately, repairing or replacing damaged organs.

Table 7 AM Technologies Proprieties

2.4 PEGDA: structure and properties

Poly(ethylene glycol) diacrylate (PEGDA) is a polymer obtained by the polymerization of ethylene glycol diacrylate (EGDA). Ethylene glycol diacrylate is a diacrylate derivative of ethylene glycol, which has two acrylate groups (-CH2=CHCOO-) attached to the two ends of the ethylene glycol molecule.Poly(ethylene glycol) diacrylate is commonly used in the field of polymer chemistry as a crosslinkable resin. The acrylate groups in PEGDA can undergo radical polymerization reactions, which allows PEGDA to be crosslinked with other polymers or monomers to form networks or polymers with desired properties.

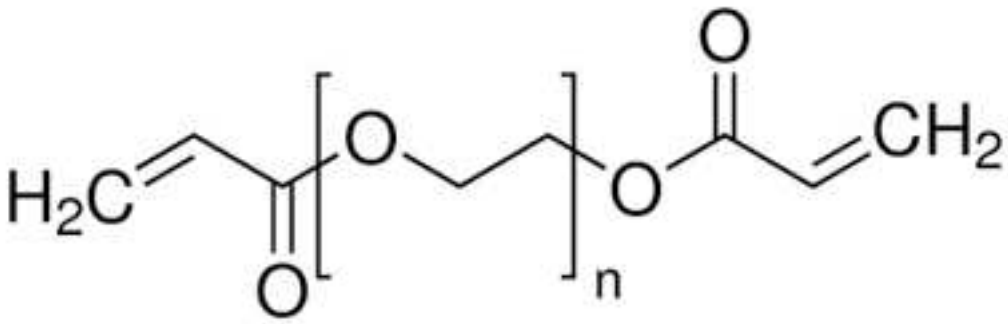

Figure 15 PEGDA Structure

The length of the PEG chain (denoted by *n*, typically ranging from about 1 to 500 ethylene oxide units) can be adjusted, giving PEGDA molecular weights from a few hundred to several thousand daltons. Lower-molecular-weight PEGDA, which contains shorter PEG segments, forms tightly crosslinked, dense polymer networks, whereas higher-molecular-weight PEGDA produces softer, more elastic hydrogels with higher swelling capacity. By varying PEGDA molecular weight and concentration, formulators can finely control the crosslink density and mechanical modulus. The PEG backbone imparts water solubility and biocompatibility, allowing even high-molecular-weight PEGDA to dissolve or disperse easily in aqueous systems.

Beyond biocompatibility, the mechanical attributes of a polymeric matrix are equally important and should be designed to address the requirements of the tissue being replicated. The compressive modulus and other mechanical attributes of crosslinked hydrogel materials can vary greatly. In choosing materials that have desirable, intrinsic mechanical properties, one can alter the processing conditions during polymerization or combine various polymers to achieve a final biomaterial with desired mechanical characteristics. By changing the ratio of the low and high molecular weight components in a polymer blend, we can control the mechanical properties of the polymer matrix (Mazzoccoli JP, 2010).

An important biologic feature is the low toxicity of PEGDA, which is a critical property for the design and applications of any biomaterial. This is true, even though PEGDA (unlike materials made from biological subunits) is polymerized from extremely toxic basic substances (Rekowska N, 2022).

Cured PEGDA networks are typically transparent and colorless, with a refractive index near 1.46. Their optical clarity is beneficial for photonic and microfluidic applications. Depending on crosslink density and water content, PEGDA materials can range from tough and elastic to very soft and compliant. In coatings and adhesives, even short PEGDA segments enhance flexibility and wet adhesion due to the hydrophilic, slightly tacky PEG chains. Meanwhile, the acrylate chemistry ensures the cured polymer remains solvent-resistant and dimensionally stable. To further improve strength or abrasion resistance, formulations may incorporate small amounts of multifunctional acrylates or inorganic nanofillers without compromising transparency.

2.4.1 PEGDA in biomedical applications

he first reported use of PEGDA hydrogel in biomedical applications was in the 1970s, PEGDA hydrogels were found to be biocompatible and non-toxic, making them suitable for use in cell culture studies . In the 1980 The hydrogels were found to be able to retain drugs in their pores and release them in a controlled manner over time. 1990s, PEGDA hydrogels were also used in injectable wound healing applications In the 2000s, PEGDA hydrogels were further developed for use in tissue engineering applications according to he capacity of PEGDA hydrogels to imitate the extracellular matrix (ECM) of living tissue. The hydrogels have also been used in various other applications, such as in the fabrication of micro- and nano-device (Hakim Khalili M, 2023).

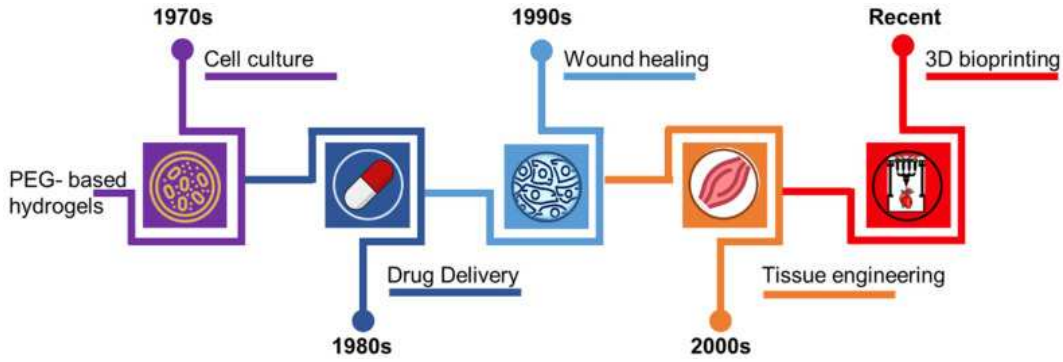

Figure 16 PEGDA-hydrogel Applications (Hakim Khalili M, 2023)

PEGDA is widely used for the fabrication of hydrogels and is often combined with other polymers such as hyaluronic acid, polyvinyl alcohol, polyether imide and maleamic acid to influence mechanical properties, stability, porosity, swelling behavior and other properties of the hydrogels. Chemical crosslinking of PEGDA with thiol-modified gelatin led to the increase in gel and thermal stability, and storage modulus (Tila Deutsch Lukatsky, 2024).

Additionally, a functionalization of PEG-based hydrogels can be achieved by adding other molecules or monomers to the hydrogel precursor solutions, for

example by including monomers generating a polyelectrolyte hydrogel. After this procedure increased protein adsorption, cell adhesion, and proliferation were observed on the functionalized hydrogels compared with the non-functionalized hydrogels. Besides enhancing cell compatibility, such polyelectrolyte hydrogels have other advantages and possible applications. Polyelectrolyte materials can be used to adsorb molecules of the opposite charge by electrostatic interaction or ion exchange and can be applied, e.g., in water purification. The choice of the monomer and its functional group is crucial for the possible application field of the hydrogel (Grübel, 2013).

Given its unique photo-crosslinking ability, PEGDA has been employed in high-precision light-based 3D printing of bone scaffolds, While PEGDA offers the flexibility for tailoring material properties (i.e., swelling capacity and mechanical strength), it lacks the inherent osteoinductive capacity unless combined with other bioactive materials .

The incorporation of a naturally derived polymer such as chitosan in composite bone scaffolds is typically characterised by enhanced biological performances such as cell adhesion and proliferation. However, chitosan is mechanically weak, therefore, it is typically combined with bioceramics or other polymers for improved properties. Among various bioceramics, hydroxyapatite is widely used for bone repair studies due to its similar chemical composition to the mineral phase of bones.. Hydroxyapatite in nanoscale size, termed nanohydroxyapatite (nHA), has reportedly induced better bioactivity and bone regeneration ability than micro-sized hydroxyapatite (Shannen Marcus Ngau, 2025).

without compromising transparency.

PEGDA is a polymer approved by the Food and Drug Administration (FDA) with good biocompatibility, which has been widely used to prepare the precursors of hydrogel MNs through photopolymerization (PEGDA shows good processability, for which a small liquid monomer can be converted into hydrogels by free radical polymerization rapidly and controllably in the presence of photoinitiators under ultraviolet (UV) light. Additionally, PEGDA can be degraded in vivo through hydrolysis of ester bonds. Consequently, PEGDA is a widely used material in

many biomedical applications, such as biosensing and drug delivery (Xinwei Fu, 2024).

2.4.2 PEGDA-based systems for bone regeneration

PEGDA-based materials generate a cross-linked three-dimensional network that serves as a physical scaffold for the adhesion, proliferation, and differentiation of osteoprogenitor cells, i.e., stem cells with osteogenic potential. This structure provides temporary mechanical support, facilitating cell colonization and the formation of new bone.

With recent developments in 3D printing technology, it has become possible to prepare scaffolds according to a predesigned (computer aided design, CAD) structure and achieve more precise control over the macroscopic structure of the scaffold.

Despite its many advantages, PEGDA is generally inelastic and brittle, which makes it more likely to be used in combination with other materials rather than alone for bone tissue engineering. It has been shown that PEGDA can be mixed with materials such as nanohydroxyapatite, nanoclay , and extracellular matrix to form bioinks for the preparation of bone tissue engineering scaffolds, which play an important role in the treatment of bone defects. However, the mechanical properties, printability, and bioactivity of these scaffolds still need to be improved (Gao, et al., 2023).

PEGDA hydrogels can mimic the physiological environment of the extracellular matrix (ECM) of living tissue in a controlled manner. This biomimetic ability promotes cell adhesion, migration, and differentiation, key elements for bone tissue regeneration.

Varying the degree of cross-linking or the chemical composition of the prepolymer it is possible to adapt the Hydrogel to the specific needs of the implant

site, ensuring an optimal balance between structural stability and biological integration.

PEGDA hydrogels can also be loaded with growth factors (such as bone morphogenetic proteins – BMP-2) or mesenchymal stem cells, serving as controlled-release systems. This approach allows for gradual and localized release of bioactive ingredients at the bone defect site, stimulating osteoinduction processes and improving the quality of newly formed tissue.

Hydrogel environment promotes osteogenesis and maturation of MC3T3-E1 cells towards an osteocytic phenotype, while the inclusion of tethered BMP-2 restricts the cells in an osteoblast differentiation state (Schoonraad SA, 2021).

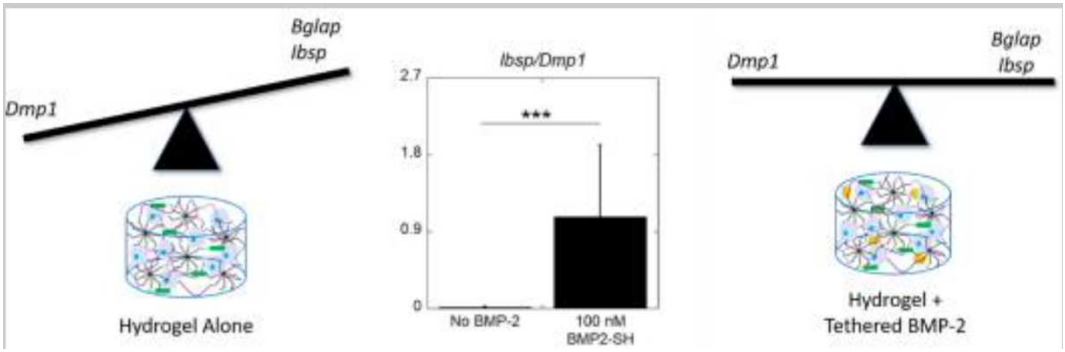

Figure 17 The different effects of the hydrogel environment without and with tethered BMP-2 on MC3T3-E1 osteogenic differentiation

2.5 Research gap and justification for 3D printing PEGDA membranes

In this context, poly(ethylene glycol) diacrylate (PEGDA) has emerged as a promising candidate for next-generation membrane fabrication. Its well-known biocompatibility, water solubility, and tunable network properties make it particularly suitable for biomedical applications where high precision and reproducibility are essential. PEGDA can be rapidly photo-crosslinked under mild conditions, enabling the creation of highly defined three-dimensional architectures with adjustable crosslink density and mechanical modulus. Modern research on PEGDA has focused only on hydrogels for tissue engineering or drug delivery, with relatively few studies exploring its potential in *membrane design for guided tissue regeneration* or other dental and biomedical applications.
Additionally, there is a lack of digital tools allowing the custom design and parametric control of membrane geometry before fabrication.
3D printing technologies, offers exceptional control over geometry, pore distribution, and material deposition, allowing researchers to fabricate reproducible PEGDA membranes with fine structural resolution.
This study addresses the current research gap by developing a dedicated software for the digital design of membrane geometries and validating its feasibility through 3D printing of PEGDA-based prototypes. This approach aims to demonstrate the potential of combining computational design and photo-crosslinkable materials to produce next-generation membranes with customizable structural and mechanical properties tailored to biomedical applications.

PART III - Design, development, and experimental validation of PEGDA membranes

"***3.1 Aim***

The purpose of this work is to establish and assess an innovative workflow that enables software-driven design and 3D printing of patient-specific, resorbable scaffolds for guided bone regeneration (GBR) in oral surgery. This design strategy allows the generation of customized membrane-like grids derived directly from the patient's CBCT dataset. The resulting virtual structures can then be produced in collagen using the Asiga Max 2 3D printing system.
The central goal of this project is to eliminate the second surgical intervention normally required to retrieve traditional titanium meshes employed in standard GBR procedures.

3.2 Materials and methods

The current phase of the larger project, to which this dissertation contributes, can be outlined through three principal components:

1. Development of a software-driven workflow for grid design
2. Evaluation and verification of the proposed methodology
3. Three-dimensional printing

Each of these components will be discussed in detail in the following sections, highlighting the key methodological steps. For clarity, several figures will accompany the description of the workflow. These examples refer to a patient exhibiting a combined vertical and horizontal defect in the first quadrant (see the section "Classification used in this study"), as illustrated in Figure 18.

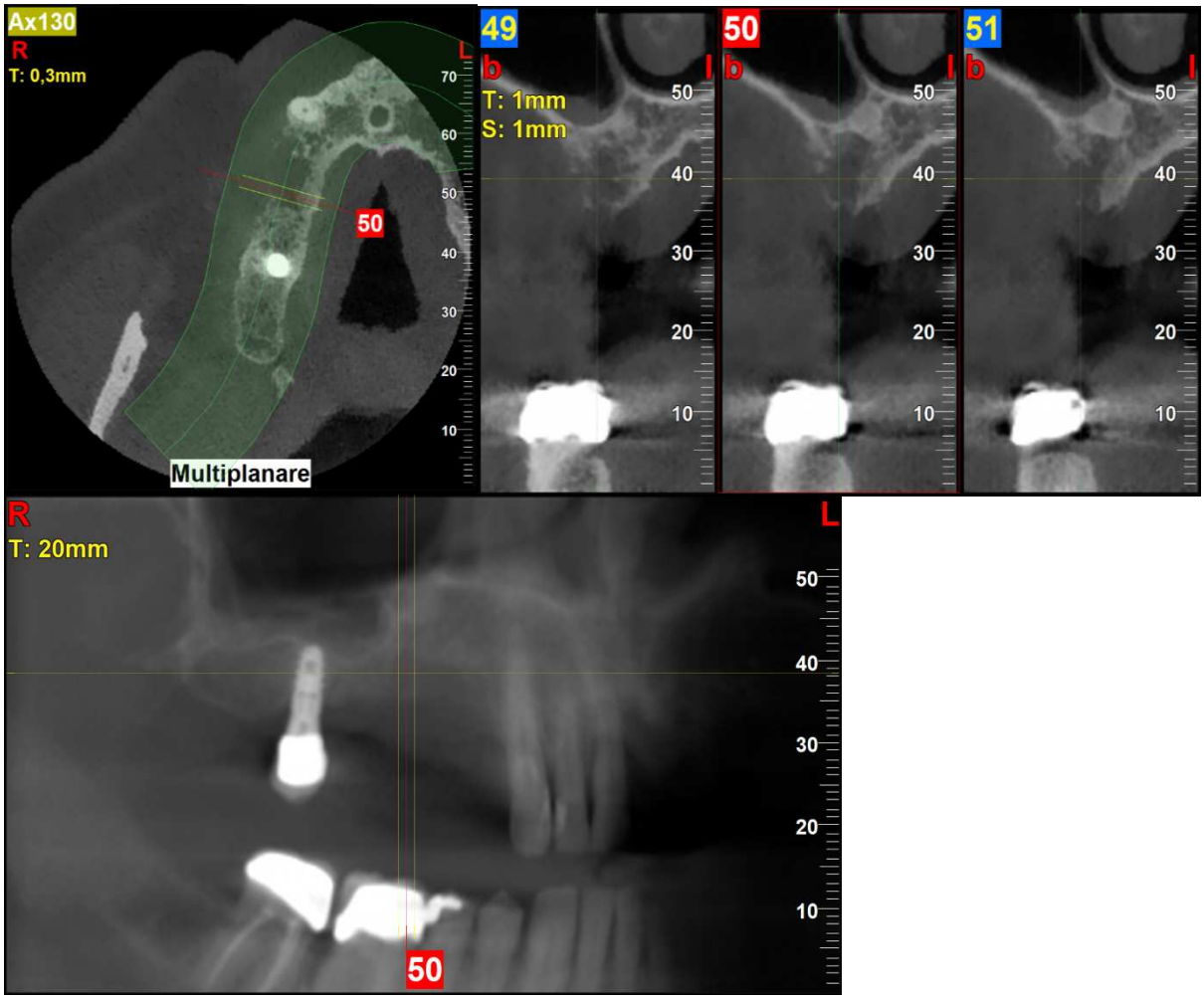

Figure 18 CBCT of a patient presenting with a combined defect in the first quadrant.

3.3.1 Software Methodology for Grid Design

The grid-design workflow developed for this project consists of several sequential steps. An initial model of both the grid and the underlying bone is generated using a custom software application developed in MeVisLab (the details of this phase are presented in the sections "Hard-tissue segmentation," "2D sectional drawing," "Interpolation," and "3D modelling"). This preliminary model is subsequently refined and modified in MeshMixer to incorporate the anchorage sites for fixation screws (see the section "Design of screw positioning"). Finally, a pre-printing verification is performed using a 3D/2D rendering tool developed in MeVisLab,

which enables the simultaneous visualization of the grid model, fixation screws, bone model, and the patient's CBCT scan within a single scene. This allows the surgeon to assess the spatial relationships between the designed structures and the patient's critical anatomical landmarks (see the section "Assessment of spatial relationships with adjacent anatomical structures").

3.3.2 Hard-tissue Segmentation

After importing the CBCT dataset, an initial segmentation is carried out using a semiautomatic Region Growing method, in which the operator selects one or more seed voxels and specifies a suitable Hounsfield-unit interval. The preliminary segmentation can then be enhanced with a dedicated refinement tool that compensates for common imaging artefacts—such as scattering or the low density of thin cortical areas—and enables the virtual removal of prosthetic elements not present during surgery.

This refinement tool permits the operator to manually "add" or "erase" voxels within the segmented region by means of a customizable brush, adjustable in both shape and size, which is applied slice by slice (see Figure 19).

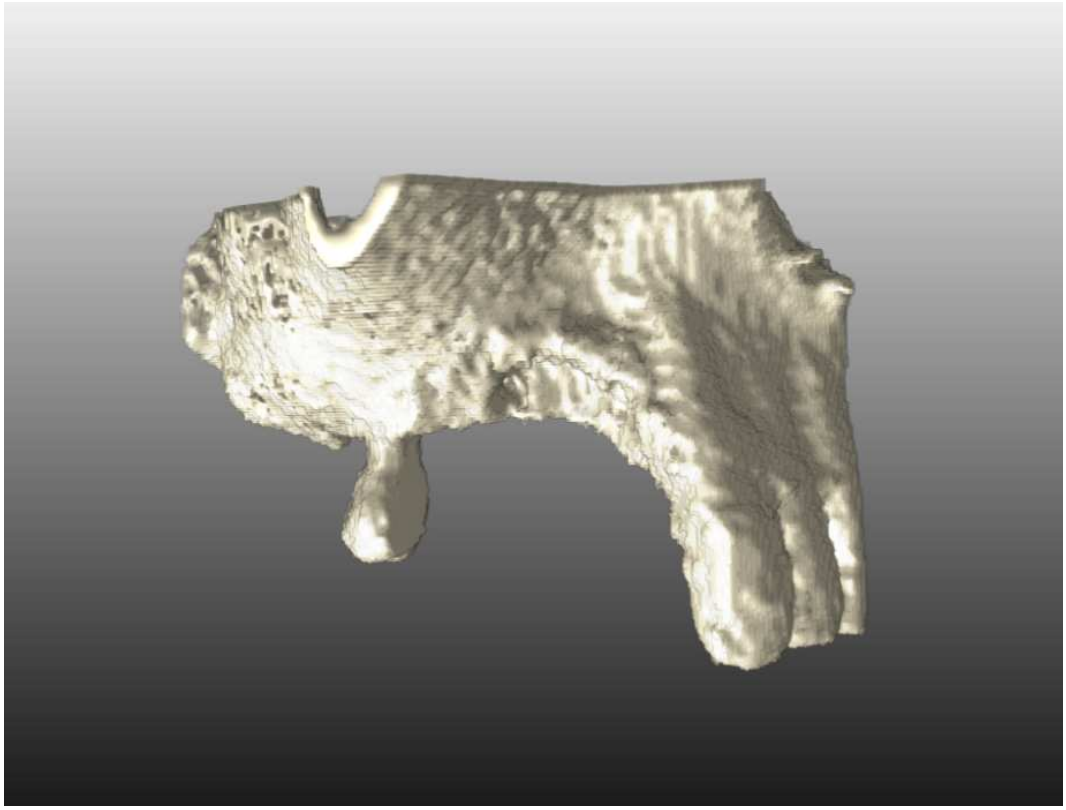

Figure 19 Hard tissue segmentation

3.3.3 2D Section Drawing

The three-dimensional shape of the membrane is produced by interpolating a series of two-dimensional contours that the operator manually traces on selected planes of interest.

The process begins by identifying the orthogonal plane that will act as the reference for constructing the 2D sections. The operator then creates multiple bidimensional outlines that, once combined, define the overall geometry of the final 3D grid. Any segments of these contours that intersect with the segmented bone surface are removed afterward.

During this stage, careful attention must be given to avoiding bony undercuts, as their presence could hinder the proper placement of the grid on the bone model in subsequent steps.

Throughout the workflow, each 2D section can be displayed directly on the 3D

segmented bone, enabling ongoing assessment of the spatial relationship between the designed profiles and adjacent anatomical structures. To further support the design process, distance-measurement tools are available to evaluate the gap between the membrane contour and the underlying bone (see Figures 20 and 21).

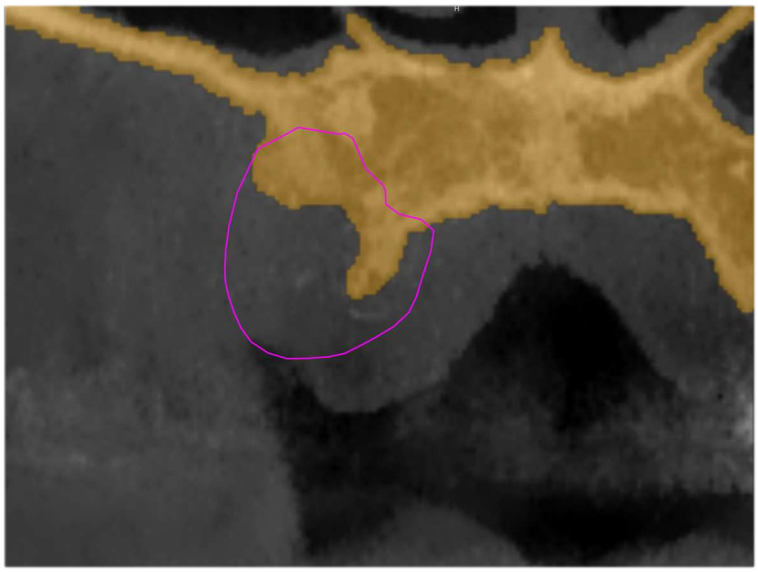

Figure 20 Bidimensional Cross-Section

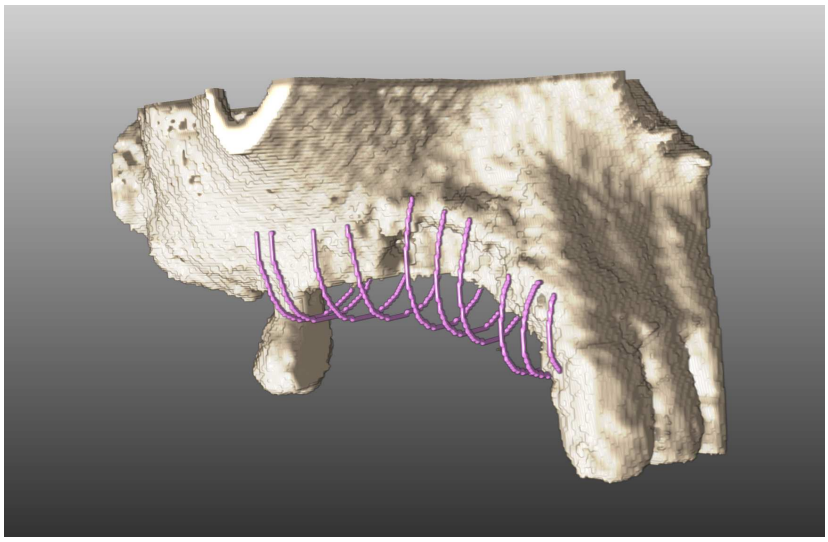

Figure 21 2D Sections on the 3D Bone Model

3.3.4 Creation of the 3D Surface

The sections produced as outlined in the previous paragraph are then processed using an interpolation algorithm. The interpolated contour is subsequently employed to construct a three-dimensional volume that represents the grid with an initial minimal thickness.

At this point, the hard-tissue model is subjected to a morphological dilation applying a spherical kernel of adjustable dimensions. The expanded bone volume is then subtracted from the thin grid model, producing a membrane shape that adapts to the patient's anatomy while preserving the required spatial separation (see Figure 22).

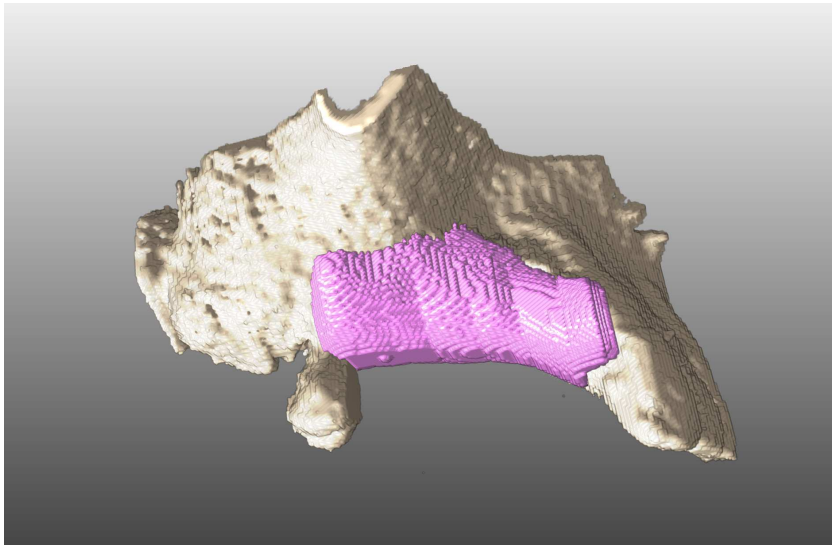

Figure 22 3D Grid Surface

3.3.5 First Draft of the Grid

By applying a morphological dilation operation using a spherical kernel of variable size to the output of the previous step, a volumetric structure is produced that serves as an initial draft of the grid. The outer surface of this preliminary model is subsequently extracted, smoothed through a refinement procedure, and exported in STL format for further processing.

3.3.6 Design of Screw Positioning

The 3D models of the grid and the segmented bone are imported into MeshMixer, where final modifications and the positioning of fixation screws are carried out. At this stage, the contour of the grid can be refined around the teeth adjacent to the defect, ensuring a clearance of approximately 2 mm between the grid and the

dental surfaces.

It is also possible to design apically oriented flanges adjacent to the neighboring teeth. These flanges may serve as stable support structures for the grid during placement. If required, the edges can be further modified to facilitate proper screw positioning and improve intraoperative handling (see Figure 23).

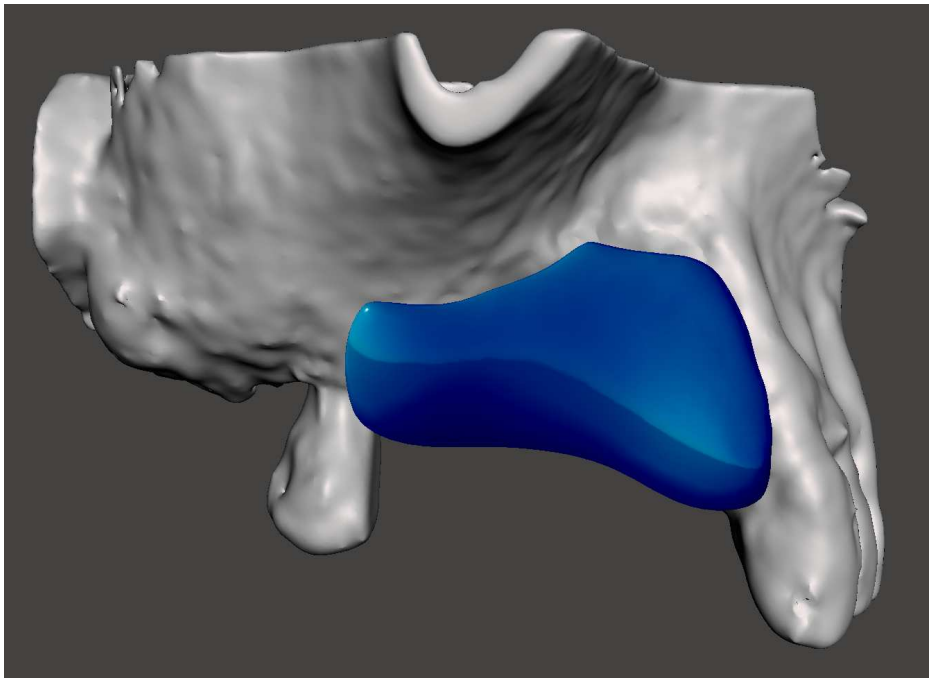

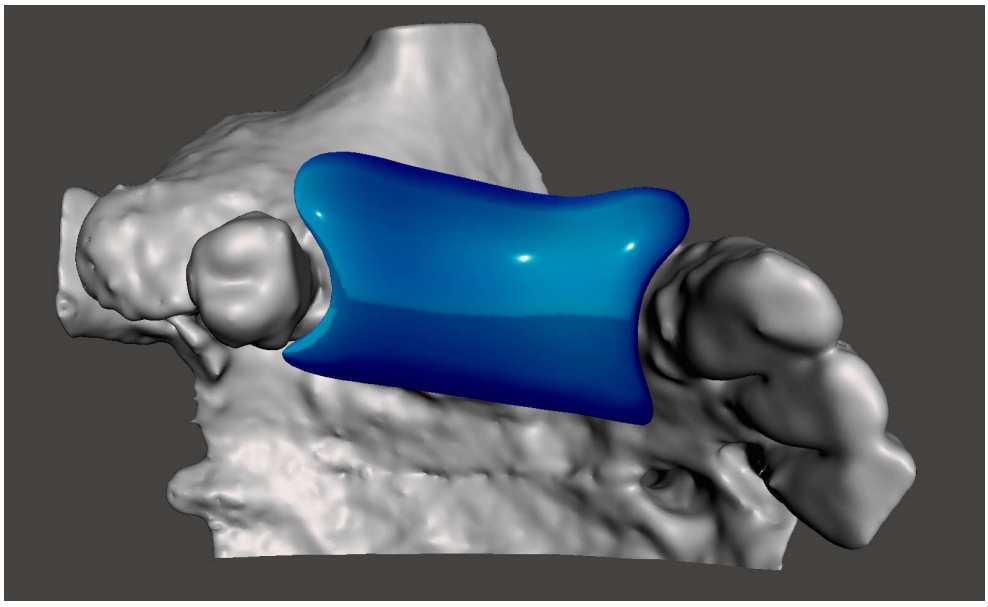

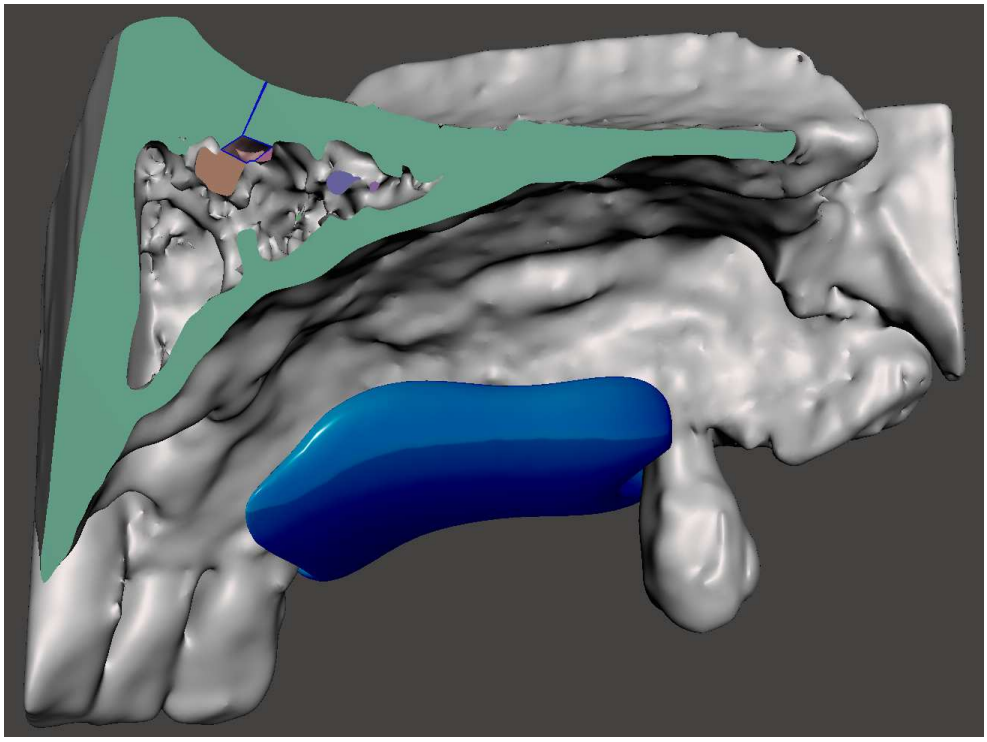

Figure 23 3D Models of the Grid and Hard Tissues

Three-dimensional models of fixation screws were created by taking as reference the screws commonly used in GBR procedures involving custom-made titanium meshes. Specifically, a screw measuring 7 mm in length and 1.35 mm in outer diameter, featuring a flat head, was selected for this study (see Figure 24).

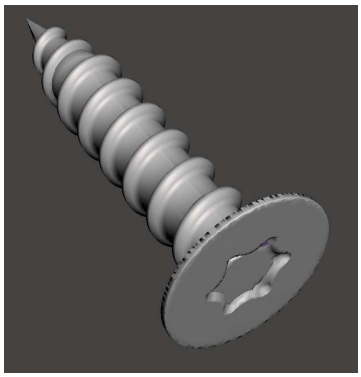

Figure 24 3D Model of fixation screw

To create the insertion holes for the fixation screws, cylindrical volumes measuring 7 mm in length and 1.40 mm in diameter were generated. The diameter

was selected slightly larger than that of the screws to facilitate smoother insertion. These cylinders were positioned so as to maintain a minimum distance of 2 mm from the edges of the grid. Naturally, screw placement must also account for critical anatomical structures, such as the inferior alveolar nerve and the roots of adjacent teeth (see Figure 25).

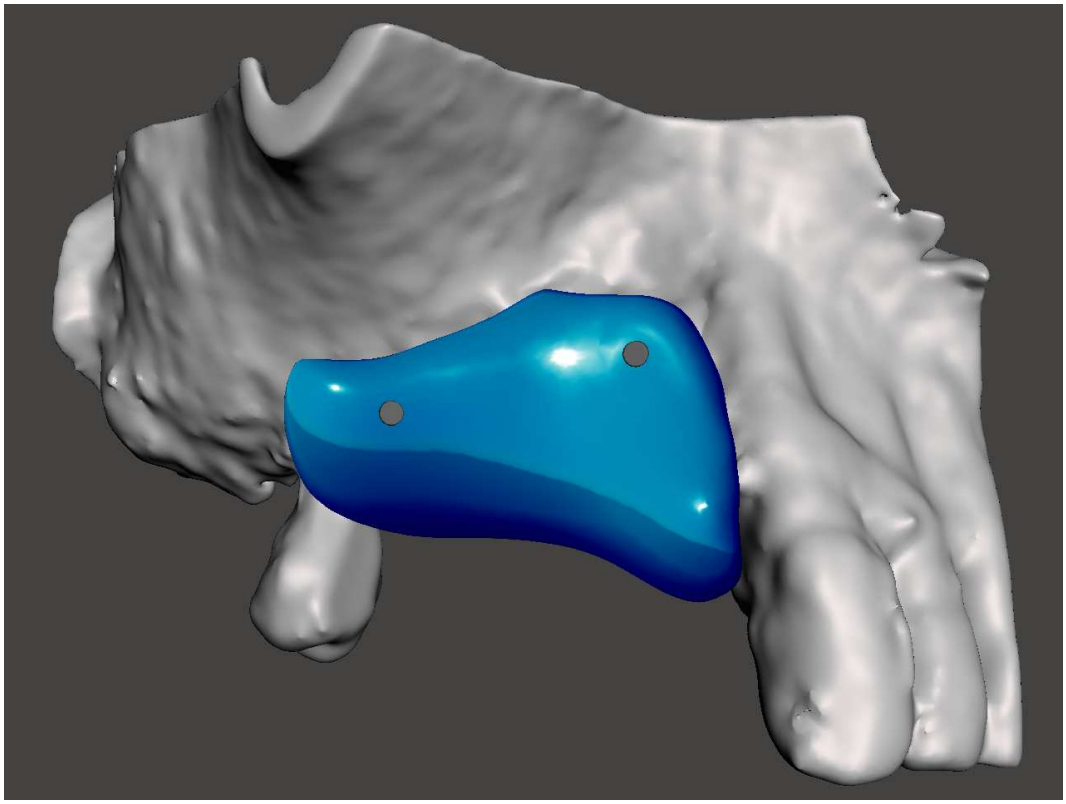

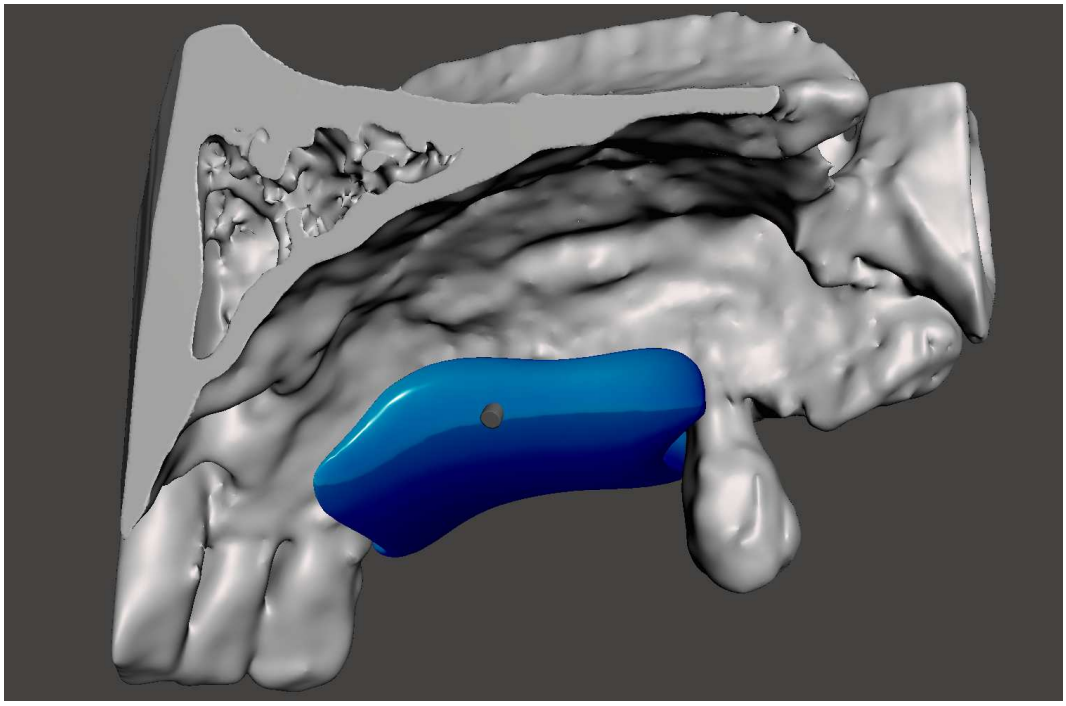

Figure 25 Grid with Cylinders

The subsequent phase consists of a remeshing process, in which the triangular mesh density of the STL model is increased locally in the areas of the grid corresponding to the cylinders. This refinement step improves the surface definition surrounding the screw-hole regions.

After remeshing, the cylinders are boolean-subtracted from the grid, creating the screw insertion openings with the necessary internal angulations to guide and seat the fixation screws (see Figure 26).

Finally, the completed grid and screw models are exported in STL format to be incorporated into the rendering tool.

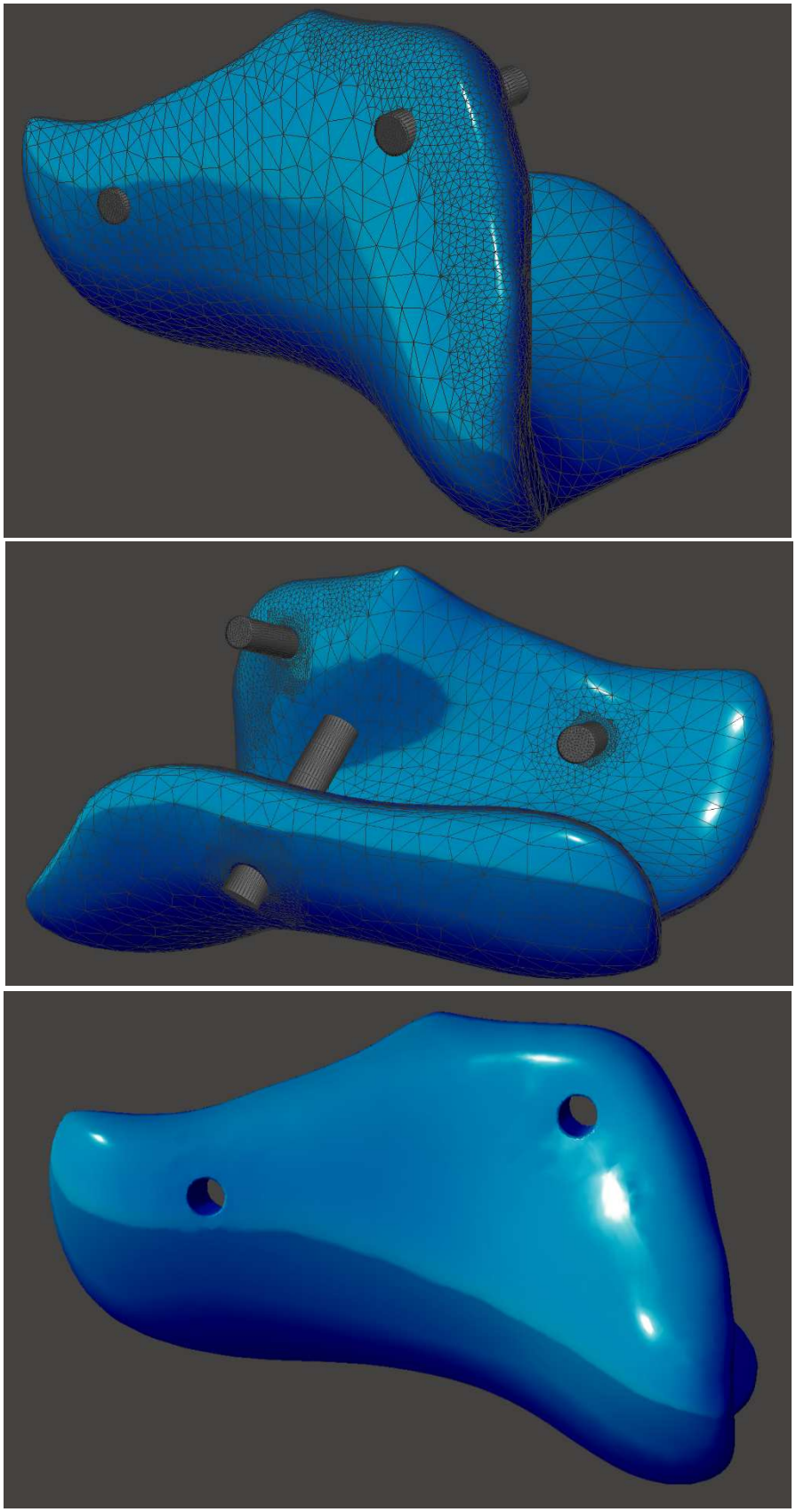

Figure 26 Grid with screw holes

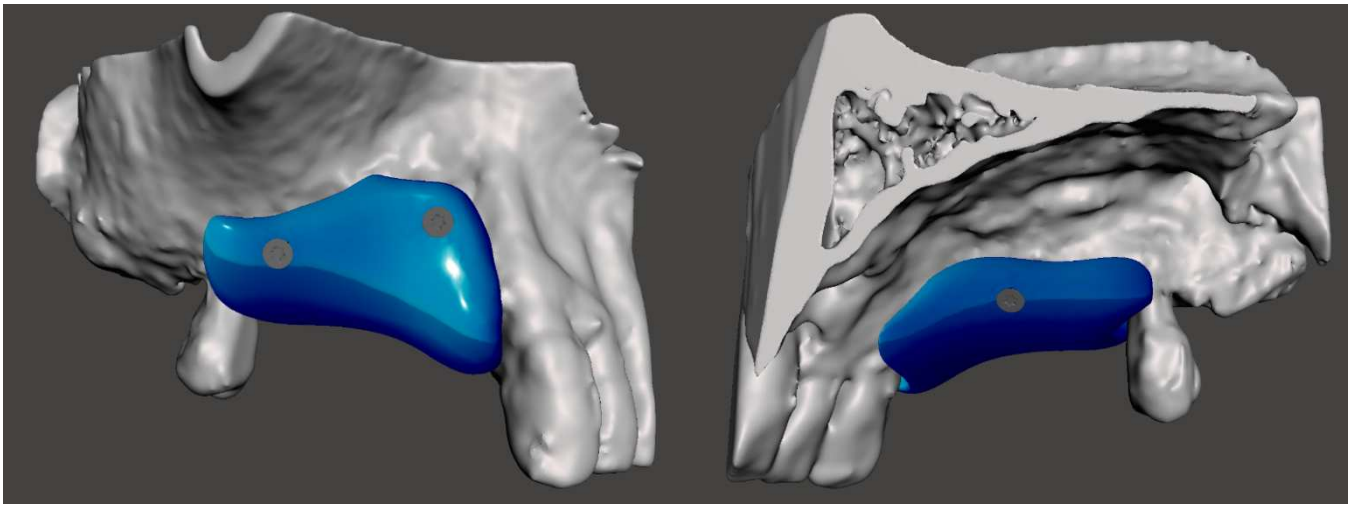

Figure 27 Final models of the hard tissues, grid, and fixation screws

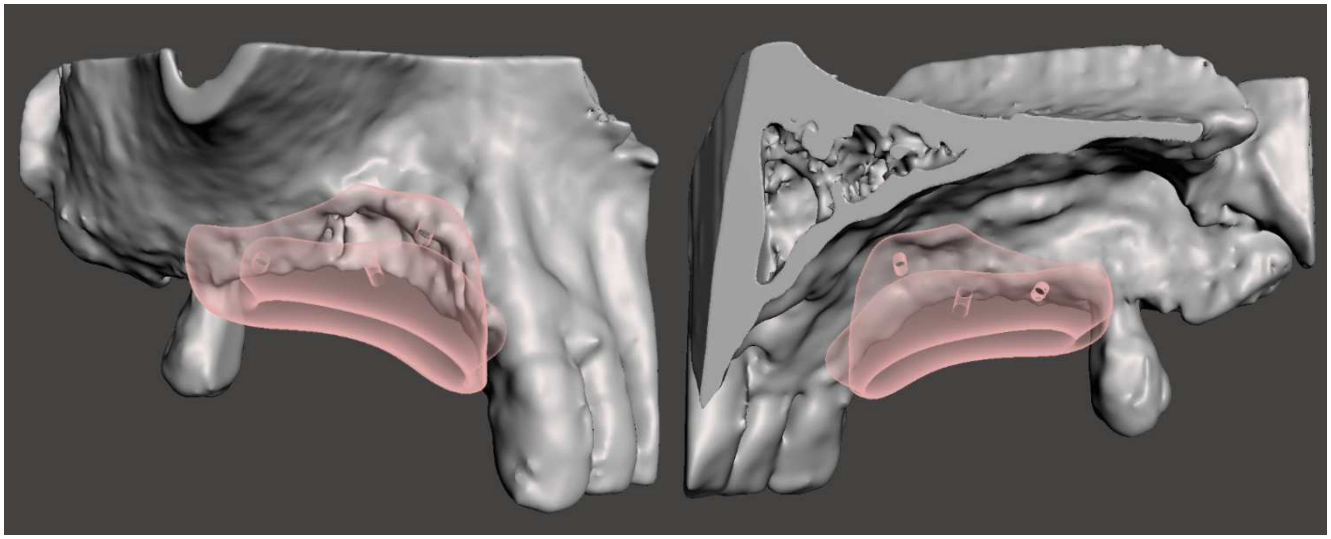

Figure 28 Transparent view of the grid superimposed on the hard-tissue model

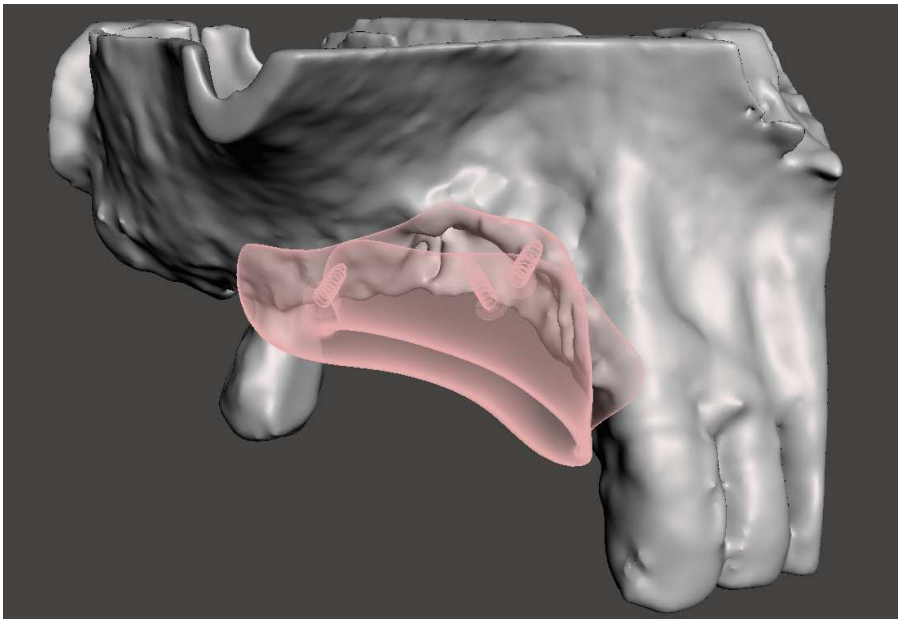

Figure 29 Transparent Rendering of the Grid and Screws

3.3.7 Assessment of Spatial Relationships with Adjacent Anatomical Structures

The files produced in the preceding phase are loaded into the rendering tool, which allows the three-dimensional models to be merged with the patient's CBCT data. This environment enables assessment of the spatial relationships between the designed elements and anatomical structures—such as the trajectories of fixation screws—through both 2D and 3D visualizations.

Within the software, a comprehensive 3D scene can be generated that includes the CBCT, screws, grid, and segmented hard tissues. Each component can be assigned adjustable transparency, permitting targeted inspection of selected structures while temporarily concealing others. The 3D environment can also be analyzed using up to six independent slicing planes, all of which can be freely

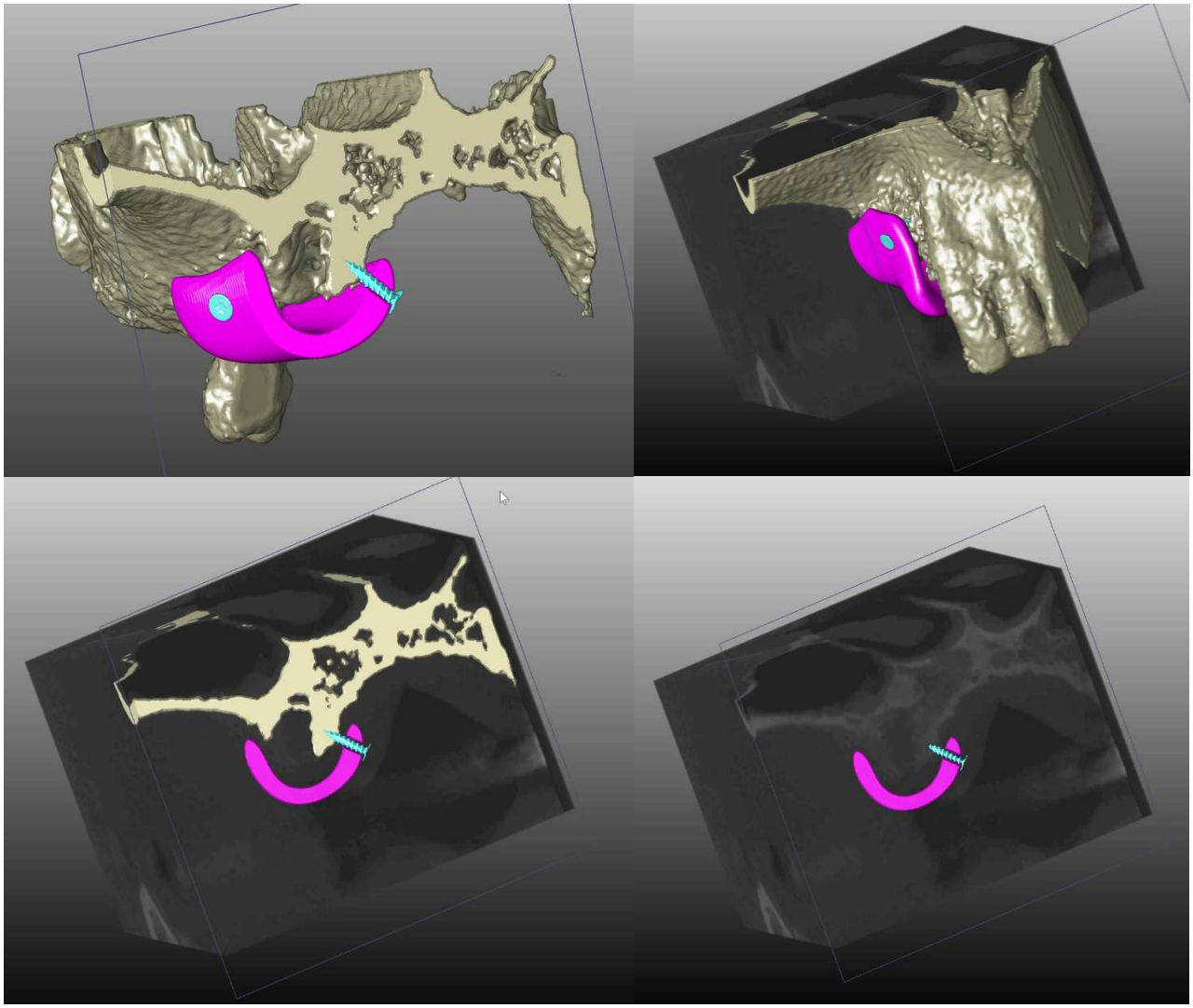

Figure 30 Rendering tool

rotated and translated in space (see Figure 30).

Two-dimensional analysis is performed using a navigation system that synchronizes the three orthogonal CBCT planes. On each plane, the grid and screws can be superimposed at varying degrees of transparency, enabling detailed verification of spatial alignment (see Figure 31).

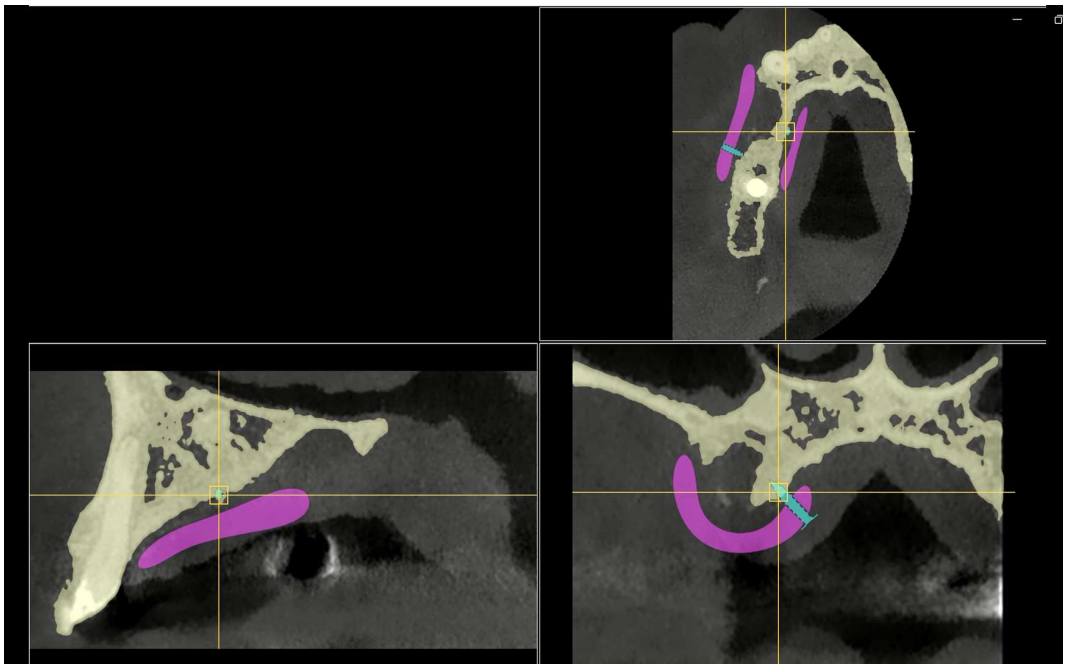

Figure 31 Bidimensional analysis

3.4 Validation of the methodology

A total of 20 patients who had undergone guided bone regeneration (GBR) with custom-made titanium meshes between 2017 and 2025, treated by the same clinician, were selected for methodological validation. These patients were classified according to the type of bone defect.

For the purposes of this study, defects were further subdivided according to their extent:

- **Small defect:** absence of one or two teeth
- **Large defect:** absence of three or more teeth

PATIENT ID	DEFECT EXTENT		DEFECT TYPE		
	Large	Small	Vertical	Horizontal	Combined
1	0	1	1	0	0
2	1	0	1	0	0
3	1	0	0	0	1
4	0	1	1	0	0
5	0	1	0	1	0
6	1	0	1	0	0
7	0	1	1	0	0
8	1	0	0	0	1
9	1	0	1	0	0
10	0	1	0	1	0
11	1	0	0	0	1
12	1	0	0	0	1
13	1	0	0	0	1
14	0	1	0	1	0
15	1	0	0	0	1
16	0	1	0	1	0
17	1	0	0	0	1
18	0	1	0	1	0
19	1	0	0	0	1
20	0	1	1	0	0
TOTALE	11	9	7	5	8

Table 8 Classification of cases used for validation

3.5 3D PRINTING

For an initial validation step, 3D prints of the hard-tissue models and the grid were produced in acrylic resin using the Formlabs 3B+ printer (see Figure 32). This printing technology is already employed clinically for the fabrication of surgical guides, providing confidence in its dimensional accuracy.
Subsequent experimental phases involve the use of the Asiga Max 2 printer (see Figure 33) to fabricate collagen-based membranes. At this stage, a first prototype of the grid was printed in PEGDA (polyethylene glycol diacrylate) to assess the feasibility of the design. PEGDA is a water-soluble, photo-crosslinkable polymer capable of forming stable polymer networks (hydrogels) when exposed to UV light in the presence of a photoinitiator.

Figure 32 Formlabs 3B+ printer
https://dental.formlabs.com/products/form-3b/

Figure 33 Asiga Max 2 printer
https://www.asiga.com/max-2/

3.6 Results

Among the 20 patients included in the methodological validation, seven displayed vertical defects, five presented horizontal defects, and eight showed combined defects. Regarding defect extent, 11 patients were classified as having large defects (≥3 missing teeth), whereas the remaining nine had small defects (1–2 missing teeth).

Seven CBCT datasets were excluded due to prosthetic restorations covering the defect area, the presence of cystic lesions, incompatibility of .KOS files with the software, or severe scattering artifacts.

Based on the CBCT scans retained for analysis, 13 customized grids were generated. These digitally designed meshes demonstrated excellent adaptation to patient anatomy, underscoring their strong suitability for GBR applications.

Two of these grids—corresponding to cases treated in 2025 with titanium mesh–assisted GBR—were further refined with the inclusion of fixation holes. One case involved a combined defect in the first quadrant, while the other presented a horizontal defect in the third quadrant. Both grids, along with their associated mandibular or maxillary models, were fabricated as resin prototypes using the Formlabs 3B+ printer.

A PEGDA prototype derived from the first case was subsequently produced to evaluate compatibility with the Asiga Max 2 printer. When positioned on the resin bone model, the PEGDA grid also demonstrated excellent anatomical correspondence.

Figures 34–37 show the resin models from the first case.

Figure 34 Lateral view of the resin-printed 3D models of the grid and hard tissues

Figure 35 Occlusal view of the models

Figure 36 Palatal view of the models

Figure 37 The resin-printed grid

Figures 38–41 show the resin models from the second case.

Figure 38 Lateral view of the resin-printed 3D models of the grid and hard tissues

Figure 39 Lingual view of the resin-printed 3D models

Figure 40 Lateral view of the resin-printed 3D models

Figure 41 3D model of the resin-printed grid

Figures 42–49 display the PEGDA-printed grid.

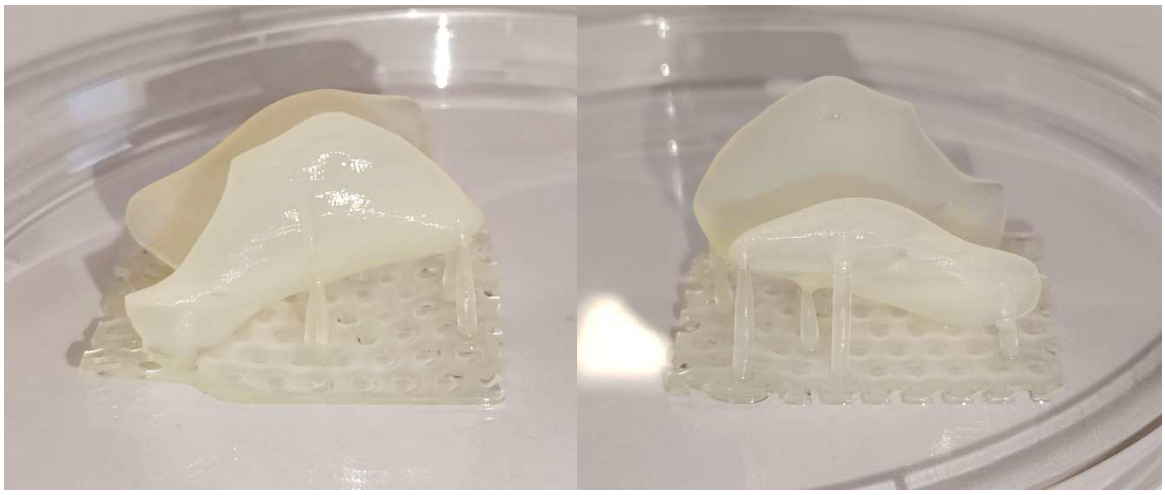

Figure 42 Buccal and palatal views of the PEGDA-printed grid with its support structure

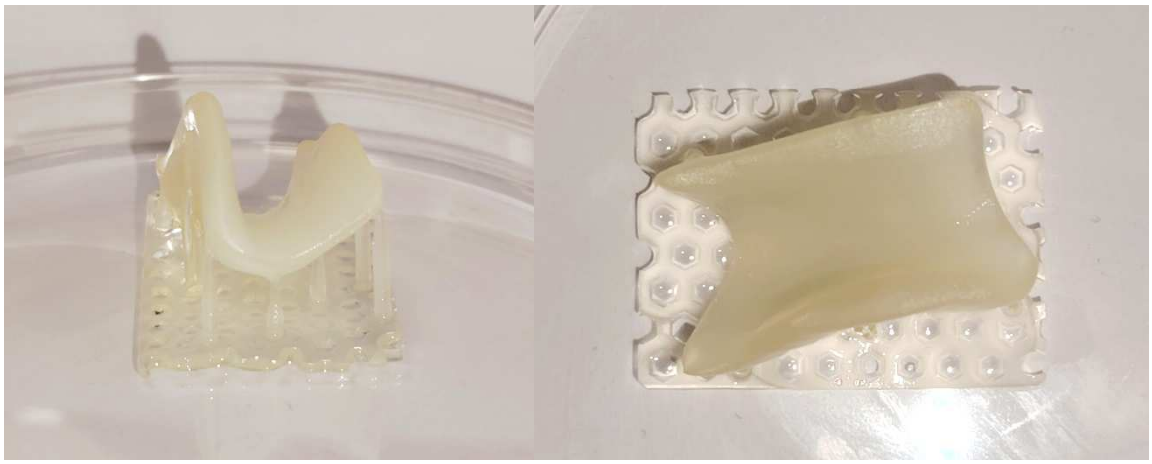

Figure 43 Mesial and internal views of the PEGDA-printed grid with its support structure

Figure 44 Buccal view of the grid

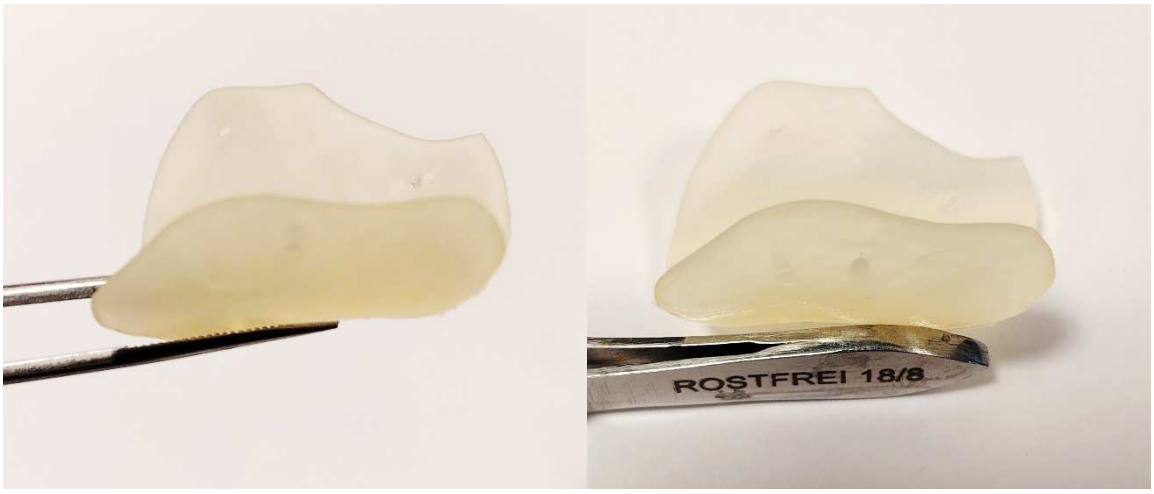

Figure 45 Palatal view of the grid

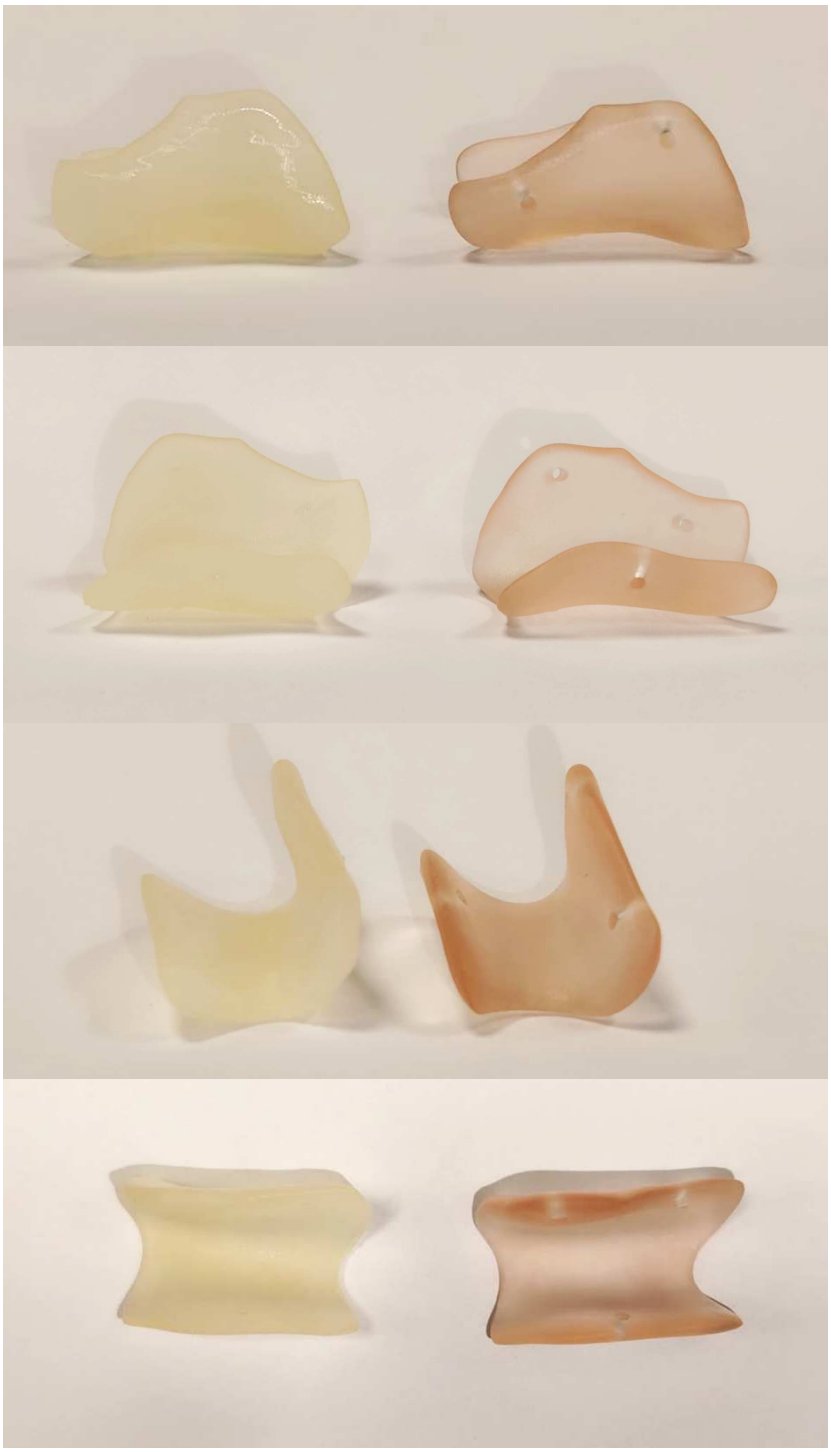

Figure 46 Different views of the grids. On the left, the PEGDA-printed grid; on the right, the resin-printed grid

Figure 47 EGDA-printed grid positioned on the resin-printed bone model. Lateral view.

Figure 48 PEGDA-printed grid positioned on the resin-printed bone model. Occlusal view.

Figure 49 PEGDA-printed grid positioned on the resin-printed bone model. Palatal view.

3.7 Discussion

Validation in 13 cases led to two primary advancements.

First, it revealed potential limitations that were subsequently addressed through the development of dedicated software tools.

The first tool enabled the selection of the most appropriate orthogonal plane for drawing the 2D sections. The sagittal plane proved most suitable for anterior defects, whereas the coronal plane was preferable for posterior defects.

A second tool allowed manual refinement of the hard-tissue segmentation by adding or removing segmented regions. This function is particularly useful in cases with excessive scattering, prosthetic elements requiring removal, or teeth scheduled for extraction. This capability allowed the recovery of a CBCT scan that was initially excluded due to poor cortical visibility and excessive noise, ultimately producing an accurate segmentation.

The screw-positioning process highlighted the necessity of a system capable of evaluating spatial relationships between patient anatomy and the designed structures. This requirement led to the development of the 3D and 2D rendering tool, which facilitated surgical planning and final verification before printing.

The second major advancement concerns improvements identified in the grid-design workflow. Three particularly relevant aspects emerged:

1. A reduced number of 2D sections results in a smoother 3D model requiring fewer refinements in MeshMixer.
2. Thoughtful selection of the section-support points reduces the risk of creating undesirable undercuts.
3. Careful design of the coronal portion of each 2D section avoids “peaks” and “saddles,” while still maintaining adequate space for bone regeneration.

3D printing also emphasized the importance of planning the insertion pathway of the grid. Improper attention to the inclination of adjacent teeth may produce a grid that theoretically fits the defect but is physically impossible to position. In the second case, careful design around adjacent teeth allowed proper placement, with insertion occurring first distally and then mesially. Poor design would have made insertion impossible.

3.8 Conclusions

This study provides a strong proof of concept for the proposed workflow, confirming its validity for the design and fabrication of patient-specific GBR devices. The software demonstrated full compatibility with the 3D printing platform intended for future clinical implementation, and the PEGDA prototype showed an excellent correspondence with the anatomical model.

The next phase of development will focus on collagen-based printing and subsequent biological testing, which are necessary steps before progressing toward a clinically deployable product.

A particularly noteworthy and innovative aspect of this approach is its potential to eliminate the secondary surgical procedure traditionally required to remove titanium meshes used in standard GBR protocols. Such an improvement could significantly reduce surgical invasiveness, operative time, and the overall physiological burden on patients.

This work was carried out in collaboration with the Health Innovation Factory (HIF) departmental development initiative, and the methodology presented herein is currently under patent review."

The present study was conducted in collaboration with Engineer Sboarina and Dr. Berfin Deveci. As a result, the iconography and the strictly technical sections related to the software development process are also included in Dr. Deveci's dissertation, entitled:

"SVILUPPO DI UN SOFTWARE PERSONALIZZATO PER LA PROGETTAZIONE E STAMPA DI CUSTOM-MADE MESH IN COLLAGENE PER ATROFIE AVANZATE DELLE OSSA MASCELLARI".

References

Al-Kattan R, R. M. (2017). Microarray gene ex-pression during early healing of GBR-treated calvarial critical size defects. *Clin Oral Implants Res*, 28:1248-1257.

Barboza EP, S. B. (2010). Guided bone regeneration using nonexpanded polytetrafluoroethylene membranes in preparation for dental implant placements--a report of 420 cases. *Implant Dent*, 19(1):2-7.

Buser D, U. I. (2023). Guided bone regeneration in implant dentistry: Basic principle, progress over 35 years, and recent research activities. *Periodontol 2000*, 93: 9-25.

Canullo L, M. V. (2008). Vertical ridge augmentation around implants by e-PTFE titanium-reinforced membrane and bovine bone matrix: a 24- to 54-month study of 10 consecutive cases. *Int J Oral Maxillofac Implants*, 23(5):858-66.

Celik HK, K. S. (2022). The state of additive manufacturing in dental research - A systematic scoping review of 2012-2022. . *Heliyon*, 9(6):e17462.

Chertok, B. W. (2013). Drug delivery interfaces in the 21st century: from science fiction ideas to viable technologies. . *Mol. Pharm.*, 3531–3543.

Chiapasco M, C. P. (2021). Customized CAD/CAM titanium meshes for the guided bone regeneration of severe alveolar ridge defects: Preliminary results of a retrospective clinical study in humans. *Clin Oral Implants Res*, 32(4):498–510.

Ciocca L, L. G. (2019). A Proposal of Pseudo-periosteum Classification After GBR by Means of Titanium-Reinforced d-PTFE Membranes or Titanium Meshes Plus Cross-Linked Collagen Membranes. *Int J Periodontics Restorative Dent*, 39(4):e157-e165.

Cirrincione, C., Guarnieri, G., & Morelli. (2025). Digital Workflow with Open-Source CAD-CAM Software Aimed to Design a Customized 3D Laser-Printed Titanium Mesh for Guided Bone Regeneration. *Bioengineering*, 12, 436.

Corinaldesi G, P. F. (2017). Histologic and histomorphometric evaluation of alveolar ridge augmentation using bone grafts and titanium micromesh in humans. *J Periodontol*, 78(8):1477–1484.

Cucchi A, G. P. (2014). Vertical Guided Bone Regeneration using Titanium-reinforced d-PTFE Membrane and Prehydrated Corticocancellous Bone Graft. *Open Dent J.* , 14;8:194-200.

Cucchi A, S. M. (2019). A Proposal of Pseudo-periosteum Classification After GBR by Means of Titanium-Reinforced d-PTFE Membranes or Titanium Meshes Plus Cross-Linked Collagen Membranes. *Int J Periodontics Restorative Dent*, 39(4):e157-e165.

Cucchi A, S. M. (2019). Histological and histomorphometric analysis of bone tissue after guided bone regeneration with non-resorbable membranes vs resorbable membranes and titanium mesh. *J Clin Implant Dent Relat Res.*, 21(4):693-701.

D. Zhao, H. D. (2022). Electrophoretic deposition of novel semi-permeable coatings on 3D-printed Ti-Nb alloy meshes for guided alveolar bone regeneration. *Dent. Mater.*, 431-443.

Dahlin. (2017). NeoGen dual texture membrane . The next generation of non-resorbable e-PTFE membranes for guided bone regeneration (GBR).
Dahlin C, L. A. (1988). Healing of Bone Defects by Guided Tissue Regeneration. *Plast Reconstr Surg*, 81(5):672–6.
Daneshmandi L, S. S.-S. (2020). Emergence of the Stem Cell Secretome in Regenerative Engineering. *Trends Biotechnol.*, 1373-1384.
Dang, M. S. (2018). Biomimetic delivery of signals for bone tissue engineering. *Bone Research*, 6, 25 .
De Santis, D. G. (2021). Digital customized titanium mesh for bone regeneration of vertical, horizontal and combined defects: A case series. *Medicina*, 57(60).
Di Stefano DA, G. G. (2019). A Preshaped Titanium Mesh for Guided Bone Regeneration with an Equine-Derived Bone Graft in a Posterior Mandibular Bone Defect: A Case Report. *Dent J (Basel)*, 1;7(3).
Elgali I, O. O. (2017). Guided bone regeneration: materials and biological mechanisms revisited. *Eur J Oral Sci*, 125(5):315-337.
Elnayef B, M. A.-M.-A. (2017). Vertical Ridge Augmentation in the Atrophic Mandible: A Systematic Review and Meta-Analysis. Int J Oral Maxillofac Implants. *Int J Oral Maxillofac Implants*, 32(2):291–312.
F., B. (2023). Exposure management of a titanium-reinforced dense polytetrafluoroethylene mesh used in a vertical ridge augmentation: A case report with 1-year follow-up. *Clin Adv Periodontics*, 13(2):84-93.
Farah Shaikh, N. L. (2023). Mesenchymal Stem Cells and Tissue Engineering in Dentistry. *intechopen*.
Franceschi, R. T. (1093–1103). Biological approaches to bone regeneration by gene therapy. *J. Dent. Res.*, 2005.
G. Größbacher, e. a. (2023). Volumetric printing across melt electrowritten scaffolds fabricates multi-material living constructs with tunable architecture and mechanics. *Adv. Mater.*
Gabriel Mizraji, A. D. (2023). Membrane barriers for guided bone regeneration: An overview of available biomaterials. *Periodontology 2000*, 56-57.
Gao, J., Li, M., Cheng, J., Liu, X., Liu, Z., & Liu, J. (2023). 3D-Printed GelMA/PEGDA/F127DA Scaffolds for Bone Regeneration. *J. Funct. Biomater*, 14, 96.
Grübel, J. L. (2013). Preparation of multifunctional hydrogels with accessible isothiouronium groups via radical cross-linking copolymerization. *Sci Rep*, 13.
Gunatillake PA, A. R. (2003). Biodegradable synthetic polymers for tissue engineering. *European Cells & Materials*, 5(1):1-6.
Gungor-Ozkerim PS, I. I. (2018). Bioinks for 3D bioprinting: an overview. . *Biomater Sci.*, 1;6(5):915-946.
Hakim Khalili M, Z. R. (2023). Additive Manufacturing and Physicomechanical Characteristics of PEGDA Hydrogels: Recent Advances and Perspective for Tissue Engineering. . *Polymer*, 7;15(10):2341.
Haque. (2018). Secretome: pharmaceuticals for cell-free regenerative therapy In Stem Cell Drugs - a New Generation of Biopharmaceuticals. *Springer*, 17-35.

Hartmann A, H. H. (2019). Evaluation of risk parameters in bone regeneration using a customized titanium mesh: results of a clinical study. *Implant Dent.* , 28(6):543–50.

Hartmann A, S. M. (2020). Minimizing risk of customized titanium mesh exposures—a retrospective analysis. *BMC Oral Health*, 20(1):36.

He M, W. Q. (2020). Hierarchically multi-functionalized graded membrane with enhanced bone regeneration and self-defensive antibacterial characteristics for guided bone regeneration. *Chem Eng J*, 98:125542.

Hoffmann O, B. B. (2008). Alveolar bone preservation in extraction sockets using non-resorbable dPTFE membranes: a retrospective non-randomized study. *J Periodontol*, 79(8):1355-69.

Hu WJ, E. J. (2001). Molecular basis of biomate-rial-mediated foreign body reactions. *Blood*, 98:1231-1238.138.

Huan Zhou, C. L. (2019). Injectable biomaterials for translational medicine. *Materials Today*.

Huang G., W. L. (2022). Main applications and recent research progresses of additive manufacturing in dentistry. . *Biomed. Res. Int.*, 2022, 1–26.

Huang S, W. H. (2023). Additive manufacturing technologies in the oral implant clinic: A review of current applications and progress. *Front Bioeng Biotechnol.*, 20;11:1100155.

Huang Y., Z. X. (2017). D bioprinting and the current applications in tissue engineering. *Biotechnol.*, 12 (8).

Hurley LA, S. F. (1959). The role of soft tissues in osteogenesis. An experimental study of canine spine fusions. *Bone Joint Surg Am*, 41-A: 1243-1254.

Inoue BS, S. S. (2020). Bioactive bacterial cellulose membrane with prolonged release of chlorhexidine for dental medical application. . *Int J Biol Macromol*, 148:1098–108.

Javaid M, H. A. (2019). urrent status and applications of additive manufacturing in dentistry: A literature-based review. *J Oral Biol Craniofac Res.*, 9(3):179-185.

Kaya, S. B. (2025). Risk factors for dehiscence in alveolar ridge augmentation using patient-specific titanium mesh: a retrospective analysis. *nt J Implant Dent* , 11,25.

Konala. (2016). The current landscape of the mesenchymal stromal cell secretome: a new paradigm for cell-free regeneration. *Cytotherapy*, 18, 13–24.

Krishani M, S. W. (2023). Development of Scaffolds from Bio-Based Natural Materials for Tissue Regeneration Applications: A Review. *Gels*, 9(2):100.

Ku S.H., L. M. (2013). Carbon-Based Nanomaterials for Tissue Engineering. *Adv. Healthc. Mater.* , 2:244–260.

Langer R, V. J. (1993). Tissue engineering. *Science*, 260(5110).

Lee, J. S. (2020). Proteomic analysis of porcine-derived collagen membrane and matrix. *Materials (Basel)*, 13(22), 5187.

Lee, J.-Y. &.-K.-Y.-S.-G. (2010). Guided bone regeneration using two types of non-resorbable barrier membranes. *Journal of the Korean Association of Oral and Maxillofacial Surgeons.*, 36. 275.

M.C. Mateo-Sidrón Antón, F. P.-G.-G. (2025). Titanium mesh for guided bone regeneration: a systematic review. *British Journal of Oral and Maxillofacial Surgery*, 433-440.

Malchiodi L, S. A. (1998). Rigid fixation by means of titanium mesh in edentulous ridge expansion for horizontal ridge augmentation in the maxilla. *Int J Oral Maxillofac Implant.*, 13:701–705.

Mariano Sanz, C. D. (2019). Biomaterials and regenerative technologies used in bone regeneration in the craniomaxillofacial region: Consensus report of group 2 of the 15th European Workshop on Periodontology on Bone Regeneration. *Journal of Clinical Periodontology*, 82-91.

Matinlinna, J. P. (2014). Barrier Membranes for Tissue Regeneration and Bone Augmentation Techniques in Dentistry. *Singapore: Pan Stanford Publishing*.

Mazzoccoli JP, F. D. (2010). Mechanical and cell viability properties of crosslinked low- and high-molecular weight poly(ethylene glycol) diacrylate blends. *J Biomed Mater Res A.*, 93(2):558-66.

Miyamoto I, F. K. (2012). Alveolar ridge reconstruction with titanium mesh and autogenous particulate bone graft: computed tomography-based evaluations of augmented bone quality and quantity. *Clin Implant Dent Relat Res.*, 14(2):304-11.

Mojdeh Mirshafiei, H. R. (2024). Advancements in tissue and organ 3D bioprinting: Current techniques, applications, and future perspectives. *Materials & Design*, 112853.

Moro JD, B. R. (2018). Tissue engineering perspectives in dentistry: Review of the literature. *RGO-Revista Gaúcha de Odontologia*, 66:361-367.

N. Angelis, D. L. (2021). Applied sciences mechanical properties and corrosion resistance of TiAl6V4 Alloy Produced with SLM technique and used for customized mesh in bone augmentations. *Appl. Sci.*, 5622.

N. Angelis, D. L. (2022). Microscopical analysis of explanted titanium alloy customised meshes for bone augmentation : A case series study. *Discov. Mater.*, 9.

N. Annabi, e. a. (2014). 25th anniversary article: Rational design and applications of hydrogels in regenerative medicine. *Adv. Mater.*, 85-124.

N. Otawa, T. S. (2015). Custom-made titanium devices as membranes for bone augmentation in implant treatment: Modeling accuracy of titanium products constructed with selective laser melting. *J. Craniomaxillofac. Surg.*, 1289-1295.

Nasajpour A, A. S. (2018). A multifunctional polymeric periodontal membrane with osteogenic and antibacterial characteristics. *Adv Funct Mater*, 28:1703437.

Nicola De Angelis, Z. H. (2023). Bone Augmentation Techniques with Customized Titanium Meshes: A Systematic Review of Randomized Clinical Trials. *The Open Dentistry Journal*, Volume 17.

Park J. M., J. J. (2020). Dimensional accuracy and surface characteristics of 3D-printed dental casts. *J. Prosthet. Dent.*, 126 (3), 427–437.

Perić Kačarević Ž., R. P. (2019). An introduction to bone tissue engineering. *Int. J. Artif. Organs*, 43:69–86.

Pini-Prato. (2011). The Miller classification of gingival recession: Limits and draw- backs. *J Clin Periodontol*, 38: 243–245.
Potts, J. T. (311–325). Parathyroid hormone: past and present. *J. Endocrinol.* , 2015.
Q. Zhang, e. a. (2022). Shedding light on 3D printing: Printing photo-crosslinkable constructs for tissue engineering. *Biomaterials*, 286.
Qi K, C. B. (2017). Review on the improvement of the photocatalytic and antibacterial activities of ZnO. *J Alloy Compd*, 727:792–820.
Qin, L. R. (2004). Parathyroid hormone: a double-edged sword for bone metabolism. *Trends Endocrinol. & Metab.*, 60–65.
Rasia-dal Polo M, P. P. (2014). Alveolar ridge reconstruction with titanium meshes: a systematic review of the literature. *Med Oral Patol Oral Cir Bucal*, 1;19(6):e639-46.
Rekowska N, H. J. (2022). hermal, Mechanical and Biocompatibility Analyses of Photochemically Polymerized PEGDA250 for Photopolymerization-Based Manufacturing Processes. *Pharmaceutics*, 12;14(3):628.
Ren Y, F. L. (2022). Barrier Membranes for Guided Bone Regeneration (GBR): A Focus on Recent Advances in Collagen Membranes. *Int J Mol Sci*, 23(23):14987.
riella Tila Deutsch Lukatsky, Y. D. (2024). Hydrogels based on crosslinked polyethylene glycol diacrylate and fish skin gelatin. *European Polymer Journal*, 112990,.
Rispoli L1*, F. F. (2015). Surgery Guidelines for Barrier Membranes in Guided Bone Regeneration (GBR). *Journal of Otolaryngology and Rhinology*.
Robert, P. &. (1993). Biocompatibility and resorbability of a polylactic acid membrane for periodontal guided tissue regeneration. *Biomaterials*, 14(5), 353–358.
Rodríguez-Lozano FJ, I. C.-H. (2012). Mesenchymal dental stem cells in regenerative dentistry. *Medicina oral, patologia oral y cirugia bucal.* , 17(6):e1062.
Sabir A., A. H. (2021). Characterization of duck egg shells and bioceramic materials in making denture applications. *IOP Conf. Ser. Mater. Sci. Eng.*, 1088:012116.
Sagheb K, S. E.-N. (2017). Clinical outcome of alveolar ridge augmentation with individualized CAD-CAM-produced titanium mesh. *Int J Implant Dent*, 3(1):36.
Saquib Rouf, A. M. (2022). Additive manufacturing technologies: Industrial and medical applications. *Sustainable Operations and Computers*, 258-274.
Sasaki JI, A. G. (2021). Barrier membranes for tissue regeneration in dentistry. *Biomater Investig Dent*, 20;8(1):54-63.
Saska, S. P.-K. (2021). Polydioxanone-based membranes for bone regeneration. *Polymers*, 13, 1685.
Schoonraad SA, T. M.-2.-E. (2021). The Effects of Stably Tethered BMP-2 on MC3T3-E1 Preosteoblasts Encapsulated in a PEG Hydrogel. *Biomacromolecules*, 8;22(3):1065-1079.
Shan Y, Q. B. (2024). Biodegradable Mg-Ca/Mg-Cu bilayer membranes with enhanced mechanical, osteogenesis and antibacterial performances for GBR applications. *J Magnes Alloys*.

Shannen Marcus Ngau, K. H. (2025). 3D-printed poly(ethylene) glycol diacrylate (PEGDA)-chitosan-nanohydroxyapatite scaffolds: Structural characterization and cellular response,. *International Journal of Biological Macromolecules*, 139652,.

Son K., L. J. (2021). Comparison of intaglio surface trueness of interim dental crowns fabricated with SLA 3D printing, DLP 3D printing, and milling technologies. *Healthcare*, 9 (8), 983. .

Sultana N., H. M. (2015). Scaffolding Biomaterials. *Springer*.

T.R. Hoare, D. K. (2008). Hydrogels in drug delivery: Progress and challenges. *Polymer*, 1993-2007 .

Tanaka S, M. K. (2007). Characteristics of newly formed bone during guided bone regeneration: analysis of cbfa-1, osteocalcin, and VEGF expression. *J Oral Implantol.* , 33:321-326.139.

Tay JRH, N. E. (2022). Healing complications and their detrimental effects on bone gain in vertical-guided bone regeneration: A systematic review and meta-analysis. *Clin Implant Dent Relat Res*, 24(1):43–71.

Tessmar, J. K. (2007). Matrices and scaffolds for protein delivery in tissue engineering. *Adv. Drug Deliv. Rev.*, 274–291.

Torabi K., F. E. (2015). Rapid prototyping technologies and their applications in prosthodontics, a review of literature. *J. Dent.* , 16 (1), 1–9.

Troeltzsch M, T. M. (2016). Clinical efficacy of grafting materials in alveolar ridge augmentation: A systematic review. *J Craniomaxillofac Surg*, 44(10):1618–1629.

Urban IA, M. E.-S. (2019). Effectiveness of vertical ridge augmentation interventions: a systematic review and meta-analysis. *J Clin Periodontol.*, 46(Suppl 21):319-339.

Vert, M. L. (1992). Bioresorbability and biocompatibility of aliphatic polyesters. *J Mater Sci Mater Med*, 3, 432–446.

Von Arx T, K. B. (1998). Localized ridge augmentation using a micro titanium mesh: A report on 27 implants followed from 1 to 3 years after functional loading. *Clin Oral Implant Res.*, 9:123–130.

Von Arx T, K. B. (1999). Implant placement and simultaneous ridge augmentation using autogenous bone and a micro titanium mesh: A prospective clinical study with 20 implants. *Clin Oral Implant Res*, 10:24–33.

Wang HL, B. L. (2006). "PASS" principles for predictable bone regeneration. . *Implant Dent*, 15(1):8-17.

Wang, J. W. (2016). Biodegradable polymer membranes applied in guided bone/tissue regeneration: A review. *Polymers*, 8(4), 115.

Wei, H. (2022). Recent advances in smart stimuli-responsive biomaterials for bone therapeutics and regeneration. *Bone Research*, 10.

Williams, D. (2016). Biocompatibility Pathways; Biomaterials-Induced Sterile Inflammation, Mechanotransduction and Principles of Biocompatibility Control. *ACS Biomaterials Science & Engineering.*

Xie Y, e. a. (2020). Titanium mesh for bone augmentation in oral implantology: current application and progress. *J Oral Maxillofac Surg*.

Xinwei Fu, H. X. (2024). Polymer homologue-mediated formation of hydrogel microneedles for controllable transdermal drug delivery,. *International Journal of Pharmaceutics,*, 124768.

Zhou, L., Miller, J., Vezza, J., Mayster, M., Raffay, M., Justice, Q., . . . Sunkar. (2024). Additive Manufacturing: A Comprehensive Review. *Sensors*, 24, 2668.

→*Dr. Deveci's dissertation, entitled:*

"SVILUPPO DI UN SOFTWARE PERSONALIZZATO PER LA PROGETTAZIONE E STAMPA DI CUSTOM-MADE MESH IN COLLAGENE PER ATROFIE AVANZATE DELLE OSSA MASCELLARI".

→*Dr. Frensi Balliu's dissertation, entitled:*

"RIGENERAZIONE OSSEA GUIDATA CON UNA NUOVA GRIGLIA IN TITANIO CUSTOMIZZATA